Adjoint Tomography: Theory, Implementations and Applications

Qinya Liu

University of Toronto

USTC, June 2020

Traveltime tomography

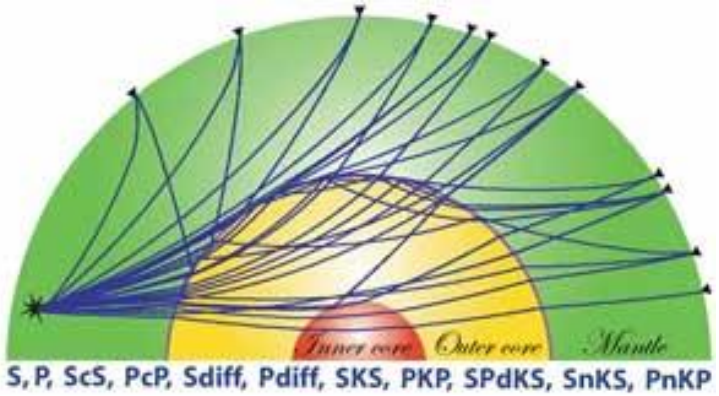

$$\Delta T = \int_{\text{Ray}} s \, dl$$

Ray theory（射线理论）
High-f approximation

Collect all types of data from all events

$$\begin{bmatrix} \Delta T_1^{\text{event-1}} \\ \Delta T_2^{\text{event-1}} \\ \vdots \\ \Delta T_j^{\text{event-2}} \\ \Delta T_{j+1}^{\text{event-2}} \\ \vdots \\ \vdots \\ \Delta T_N^{\text{event-n}} \end{bmatrix} = \begin{bmatrix} K_{11} & K_{12} & \cdots & K_{1M} \\ K_{21} & K_{22} & \cdots & K_{2M} \\ & \vdots & \vdots & \\ & \cdots & \cdots & \\ & \vdots & \vdots & \\ & \vdots & \vdots & \\ & \vdots & \vdots & \\ K_{N1} & K_{N2} & \cdots & K_{NM} \end{bmatrix}$$

1	2	3	4	5	6	7	8
9	10	11	etc.				
17							
25							

$$\begin{bmatrix} s_1 \\ s_2 \\ \vdots \\ s_M \end{bmatrix}$$

* for ray theory, K_{ij} is the length of the ray in the M'th block for the I'th data

$$d = Gm$$

LSQ inversion with regularization

$$m_{\text{est}} = \left[G^T G + \lambda L(m)\right]^{-1} G^T d$$

Finite-frequency Tomography

Cross-correlation traveltime

$$\delta T = \int_V K_m(\mathbf{x})\, d\ln m(\mathbf{x})\, d\mathbf{x}$$

$$\begin{bmatrix} \Delta T_1^{\text{event-1}} \\ \Delta T_2^{\text{event-1}} \\ \vdots \\ \Delta T_j^{\text{event-2}} \\ \Delta T_{j+1}^{\text{event-2}} \\ \vdots \\ \vdots \\ \Delta T_N^{\text{event-n}} \end{bmatrix} = \begin{bmatrix} K_{11} & K_{12} & \cdots & K_{1M} \\ K_{21} & K_{22} & \cdots & K_{2M} \\ & \vdots & \vdots & \\ & \cdots & \cdots & \\ & \vdots & \vdots & \\ & \vdots & \vdots & \\ & \vdots & \vdots & \\ K_{N1} & K_{N2} & \cdots & K_{NM} \end{bmatrix} \begin{bmatrix} s_1 \\ s_2 \\ \vdots \\ s_M \end{bmatrix}$$

Sensitivity kernels（地震数据的敏感核）

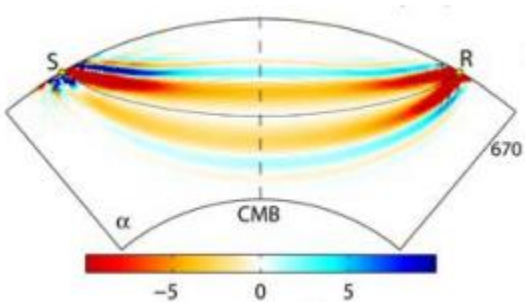

Finite-frequency kernels

Based on Born Approximation
(i.e., single scatter approx)

$$K_m(\mathbf{x}) \sim \int_0^T s(\mathbf{x},t)\cdot s^{\dagger}(\mathbf{x},T-t)\,dt$$

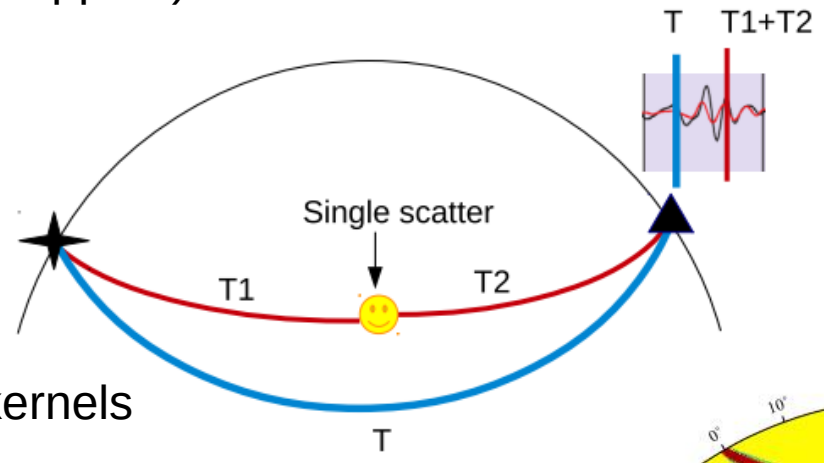

Ray theory:
Banana-doughnut kernels
(Dahlen et al 2000,
Hung et al, 2000)
difficulty with diffracted phase

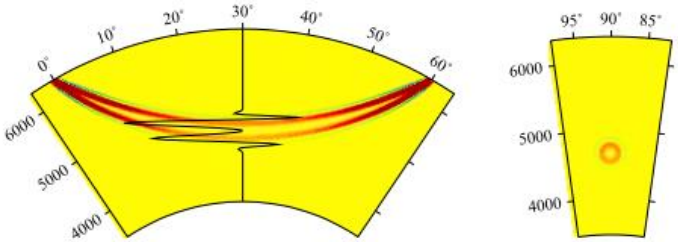

Normal Modes: 1D models
(Zhao et al 2000,
Zhao & Jordan 2006)

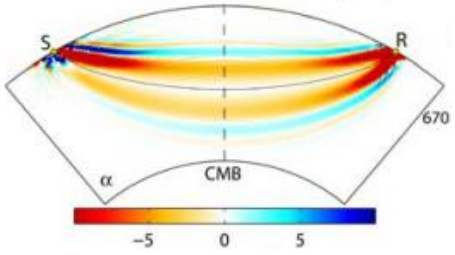

Surface wave mode summation:
(Zhou et al, 2004,2008)

Numerical wave simulations (Liu & Tromp
2006,2008, Nissen-Meyer 2007)

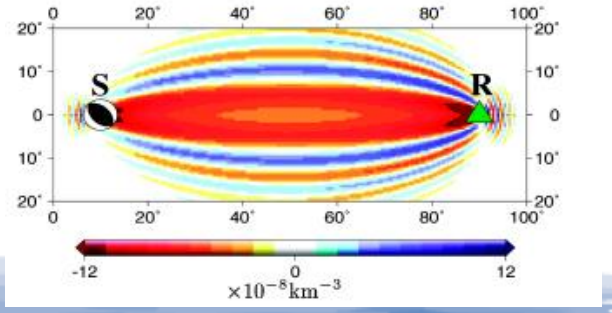

Finite-frequency tomography 有限频层析成像

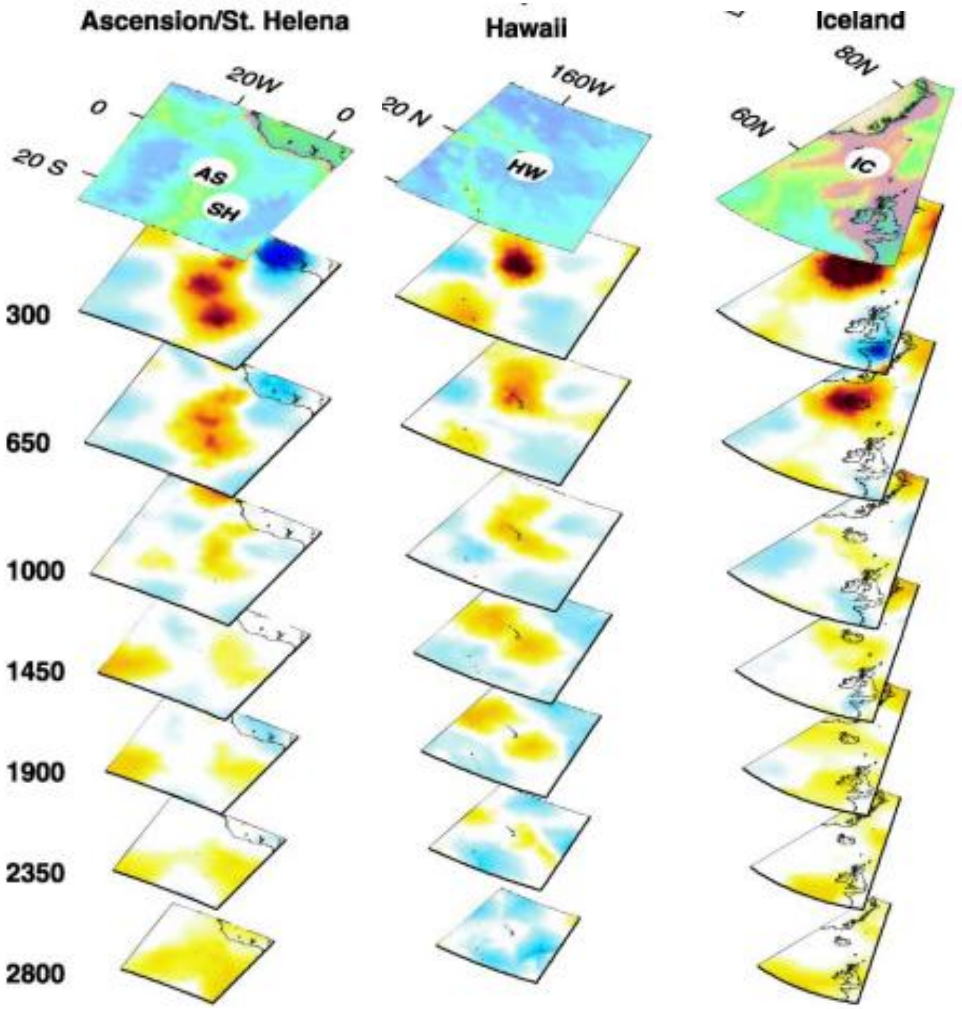

Montelli et al 2004 (Science)

Liu & Gu 2012

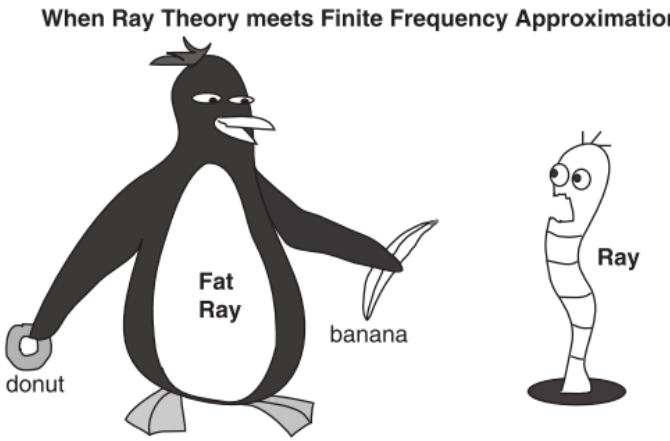

Ray vs. Finite-frequency kernel debate

*Dahlen and Nolet, 2005; Montelli et al., 2006a
* de Hoop and van der Hilst, 2004; van der Hilst and de Hoop, 2005, 2006

<u>Effect of regularization/smoothing</u>

Other finite-frequency tomography studies: Hung et al 2006, 2008, 2010
Obrebski et al 2011, 2012, 2014, etc

How to further improve seismic imaging

- *More seismic data* (improved coverage):
  * more earthquake data, seismic array data
  * ambient noise data, scattered waves
  * waveform, frequency-dependent measurements

- *more accurate sensitivity kernels* K_m(x)
  * accurate Green's functions → normal mode for 1D (Zhao & Chevrot 2011), numerical simulations for 1D (Nissen-Meyer et al 2007) and 3D models (Liu & Tromp 2006, 2008)
  * ambiguity from regularization still exists

- *Iterative inversion for a nonlinear inverse problem*
  * accurate 3D Green's functions, sensitivity kernels → 3D numerical solvers
  * full waveform inversion (FWI, Tarantola 1984) / adjoint tomography (Tromp et al 2005)　全波形反演 / 伴随层析成像

Adjoint tomography: 3D numerical solvers

- Finite difference
- Finite element
- Spectral element

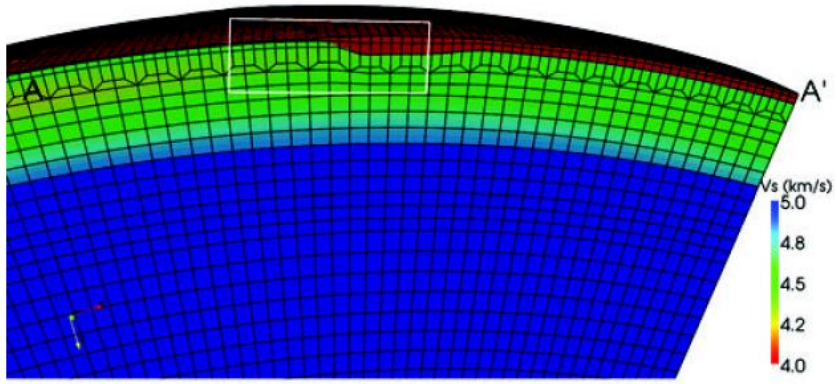

SPECFEM3D_GLOBE
Komatitsch & Tromp (2002 a, b), Tromp et al (2010)

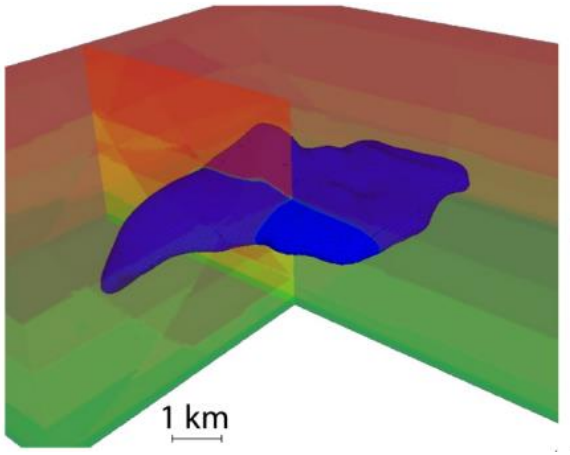

SPECFEM3D,
Komatitsch et al (2004), Peter et al (2011)

Advantages:

* Weak formulation → topography, internal surfaces, complex geology
* Interpolation/integration of wavefield on local GLL points → diagonal mass matrix
* Meshing by doubling schemes → efficient
* Diagonal mass matrix, local communications → Parallel computation
* Community-supported/developed, open-source; GPU-enabled.

Computational Infrastructure for Geodynamics (CIG):
http://www.geodynamics.org/cig/software/packages/seismo/

Local/Global Sensitivity Kernels

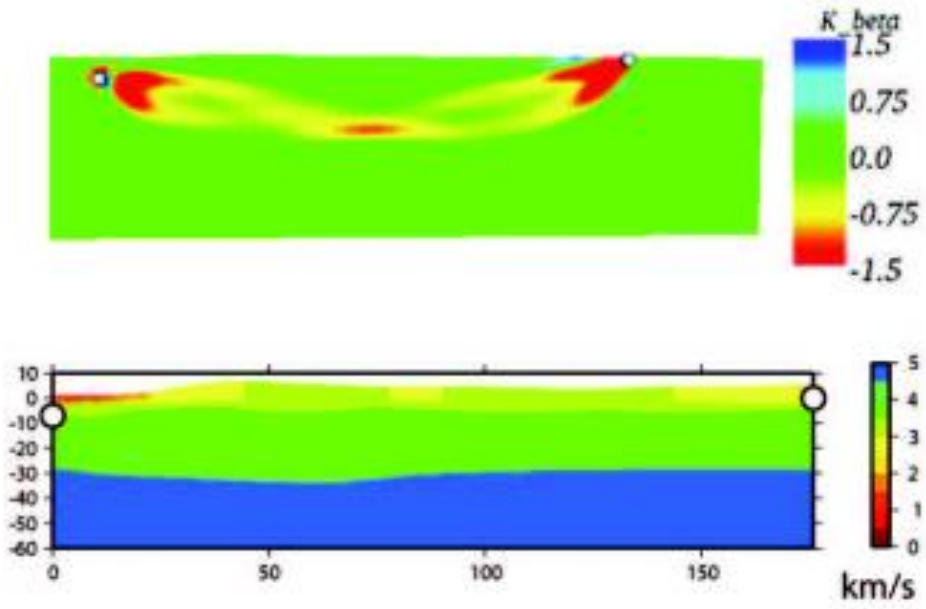

SPECFEM3D package,
SmS/Sn waves
(Liu & Tromp 06)

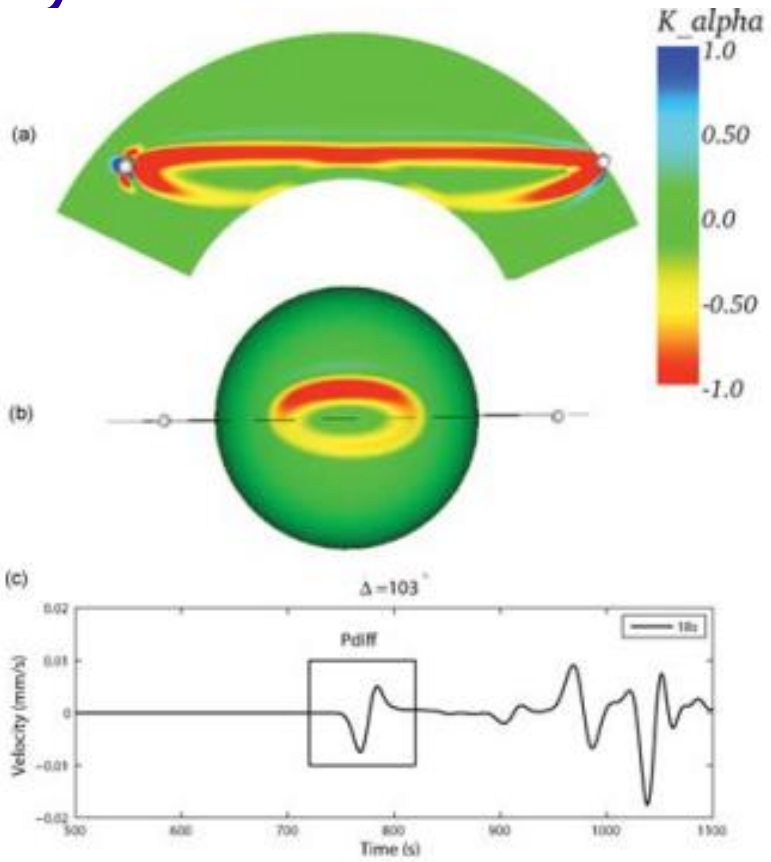

SPECFEM3D_GLOBE package,
Pdiff kernels (Liu & Tromp 08)

Two main advantages

1. Works on 3D reference models!

2. No prerequisite knowledge on the pulses measured.

Disadvantage: numerically expensive!!

Nonlinear Inverse problem

Misfit function $$\phi(m) = \sum [T(m) - T_{obs}]^2 = \sum \Delta T^2$$

Gradient vector $$\frac{\partial \phi}{\partial m} = \sum \frac{\partial T}{\partial m} \Delta T$$

Data assimilation
Adjoint field

We already know how to compute

$$\frac{\partial T}{\partial m} \sim \int s(x,t) \cdot s^{\dagger}(x, T-t)\, dt$$

Event kernel (gradient) $$\frac{\partial \phi_e}{\partial m} \sim \int s(x,t) \cdot s^{\dagger}_{\text{event}}(x, T-t)\, dt$$

Two numerical simulations ..

Unfortunately, computing the 2nd order derivative, i.e, the Hessian matrix H = G^T G is too costly

Traditional Tomography (Ray, FF) $H \Delta m = -g$ Gauss-Newton Method

Adjoint tomography $\phi(m^j),\ g = \frac{\partial \phi}{\partial m}(m^j)$ Iterative nonlinear inversions

Adjoint tomography: Examples

We take the adjoint tomography of Europe (Zhu et al 2015) as an example. This is a comprehensive study that can be considered the paradigm of adjoint tomography.

Here is a key summary:

* 190 earthquakes, 745 stations
* initial model: Epcrust + S360ANI (called EU00)
* source inversions: centroid moment tensor and locations
* adjoint tomographic inversions in three stages
  ** stage 1: T(f) --> radially anistropic parameters
  ** stage 2: T(f), A(f) --> elastic parameters + anelastic parameters
  ** stage 3: T(f), A(f) --> radial and azimuthal anistropy
  Note: first two stages uses long-period surface wave (50/20-150 s) + short-period body waves (15-50 s), and the last stage uses only surface waves.
  ** after 60 iterations --> EU60

Study Area: Events & Stations

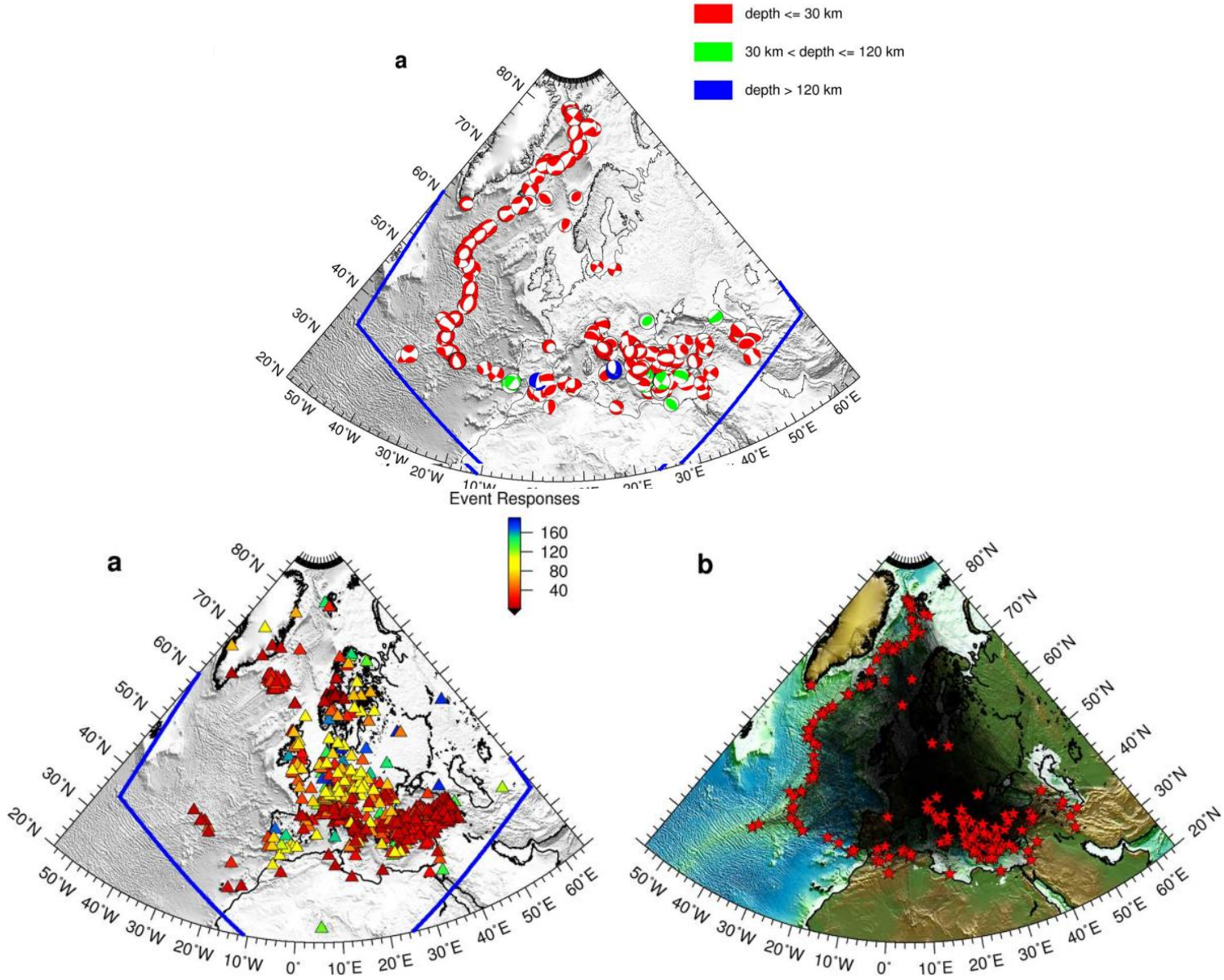

Initial model: Moho

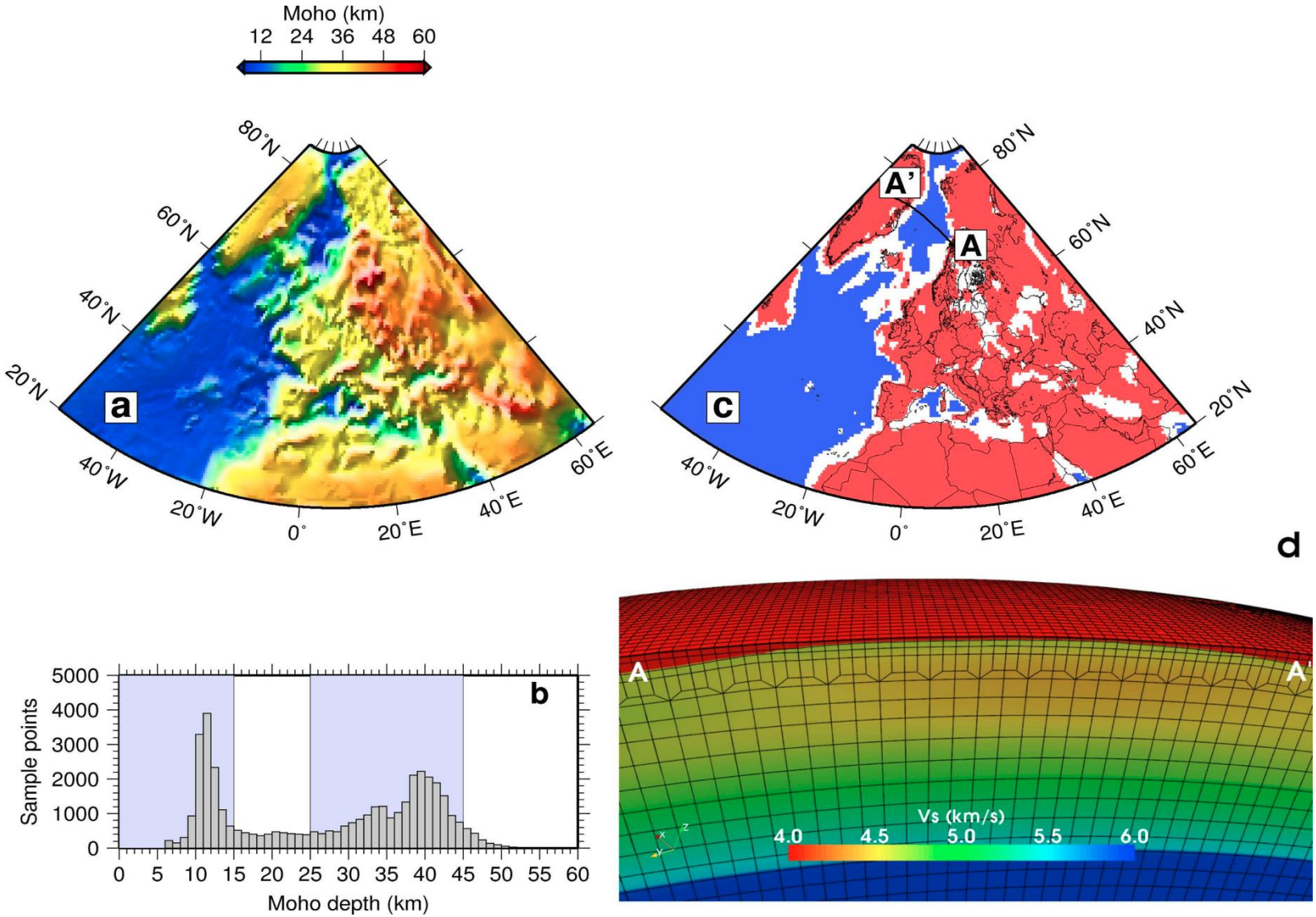

Moho is honored by one layer element when d < 15 km, 2-3 layer of elements when d is between 25-45 km.

Initial model: S362Ani

1D radially Anisotropic Model:

STW105

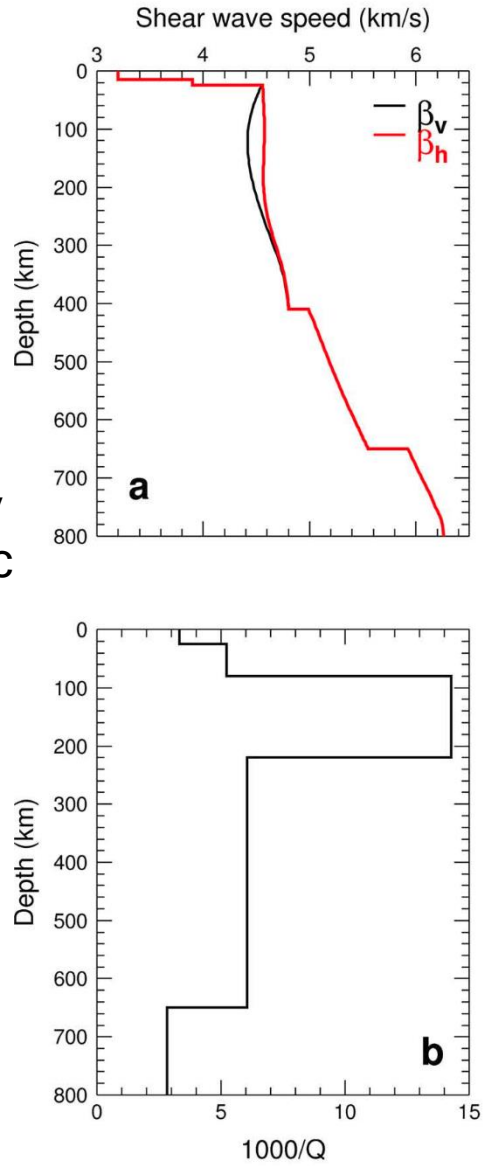

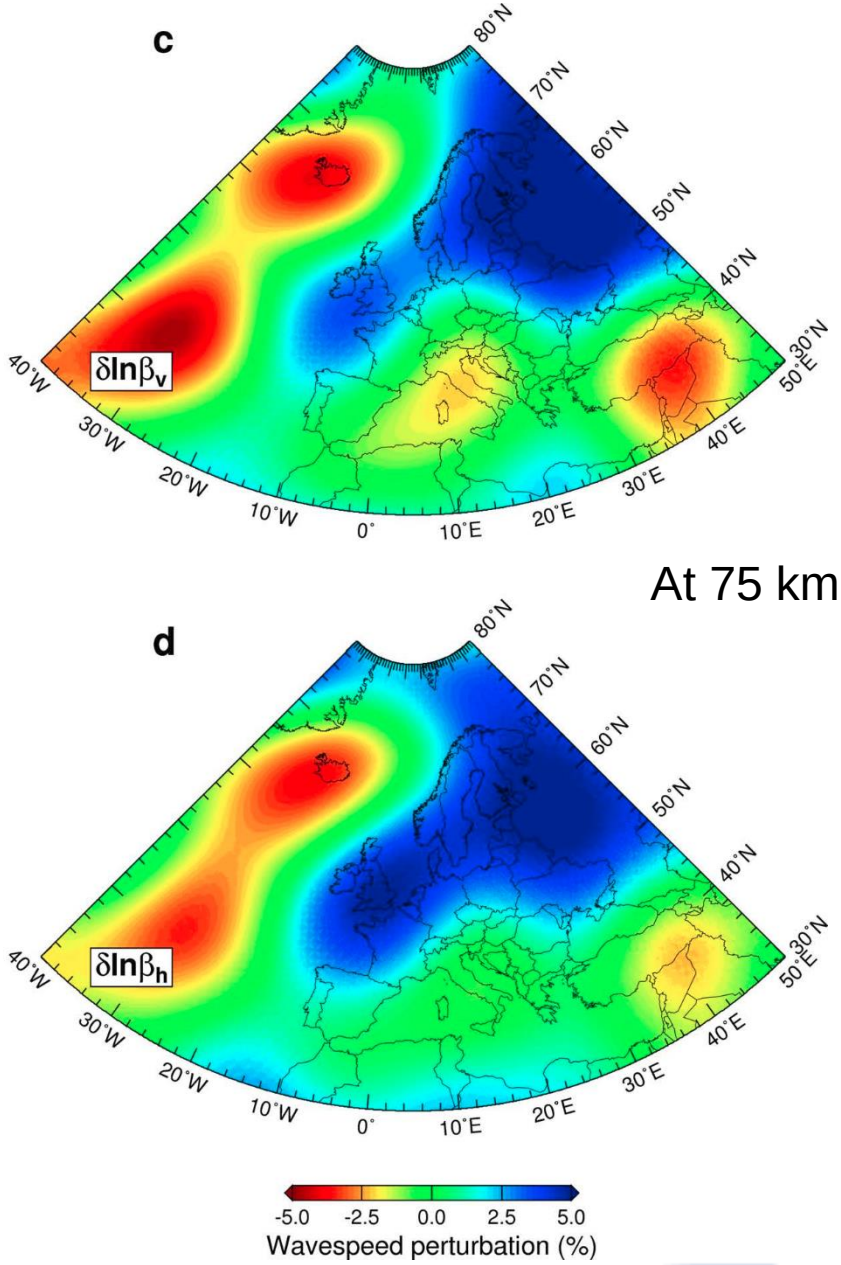

At 75 km depth

Stage I: Inversion Steps

Define misfit function

$$\chi_{\mathrm{I}} = \chi^{\phi}, \qquad \chi^{\phi} = \sum_{c=1}^{N_c} w_c \sum_{m=1}^{N_m} \int w_m \left[\frac{\Delta\tau_m(\omega)}{\sigma_m^{\phi}(\omega)} \right]^2 \mathrm{d}\omega,$$

Sensitivity kernels

$$\delta\chi_{\mathrm{I}} = \int_V \mathrm{K}_c\, \delta\ln c + \mathrm{K}_{\beta_{\mathrm{v}}}\, \delta\ln\beta_{\mathrm{v}} + \mathrm{K}_{\beta_{\mathrm{h}}}\, \delta\ln\beta_{\mathrm{h}} + \mathrm{K}_{\eta}\, \delta\ln\eta\, \mathrm{d}V, \qquad \delta\ln\rho = 0.33\, \delta\ln\beta, \qquad \beta = \sqrt{\frac{2\beta_{\mathrm{v}}^2 + \beta_{\mathrm{h}}^2}{3}}.$$

Preconditioner: approximate diagnonal of Hessian

$$P(\mathbf{x}) = 1 / \int \partial_t^2 \mathbf{s}(\mathbf{x}, t) \cdot \partial_t^2 \mathbf{s}^{\dagger}(\mathbf{x}, T - t)\, \mathrm{d}t,$$

Kernel smoothing (regularization)

$$\mathrm{K}(\mathbf{r}) = \frac{1}{W(\mathbf{r})} \int_V \mathrm{K}(\mathbf{r}')\, \exp[-(r'\Delta)^2/(2\sigma_{\Delta}^2)] \times \exp[-(r - r')^2/(2\sigma_r^2)]\, \mathrm{d}^3\mathbf{r}',$$

Conjugate gradient methods for nonlinear inversion

$$\mathbf{d}_i = -\mathbf{g}_i + \beta \mathbf{d}_{i-1}, \qquad \beta = \frac{\mathbf{g}_i^T \cdot (\mathbf{g}_i - \mathbf{g}_{i-1})}{\mathbf{g}_{i-1}^T \cdot \mathbf{g}_{i-1}}. \qquad \ln \frac{\mathbf{m}_{i+1}}{\mathbf{m}_i} = \alpha\, \mathbf{d}_i,$$

Alternatively, one can use other optimization techniques, e.g., Limited-memory BFGS methods

Inversion Steps (cont.)

Model update in the search direction (d is normalized)

$$\ln \frac{\mathbf{m}_{i+1}}{\mathbf{m}_i} = \alpha \, \mathbf{d}_i ,$$

Step length alpha is determined through compute misfit of a set of representative earthquakes as a function of step length (alpha = 0.01 – 0.05) corresponding to maximum 5% velocity perturbation, and monitor the reduction of misfit for all categories of data

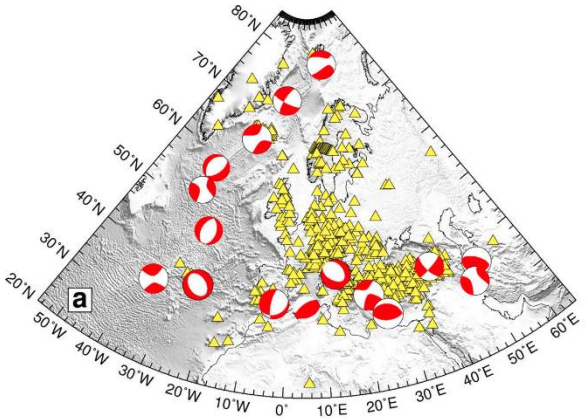

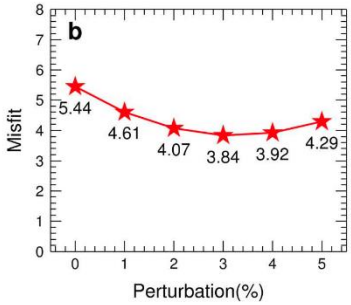

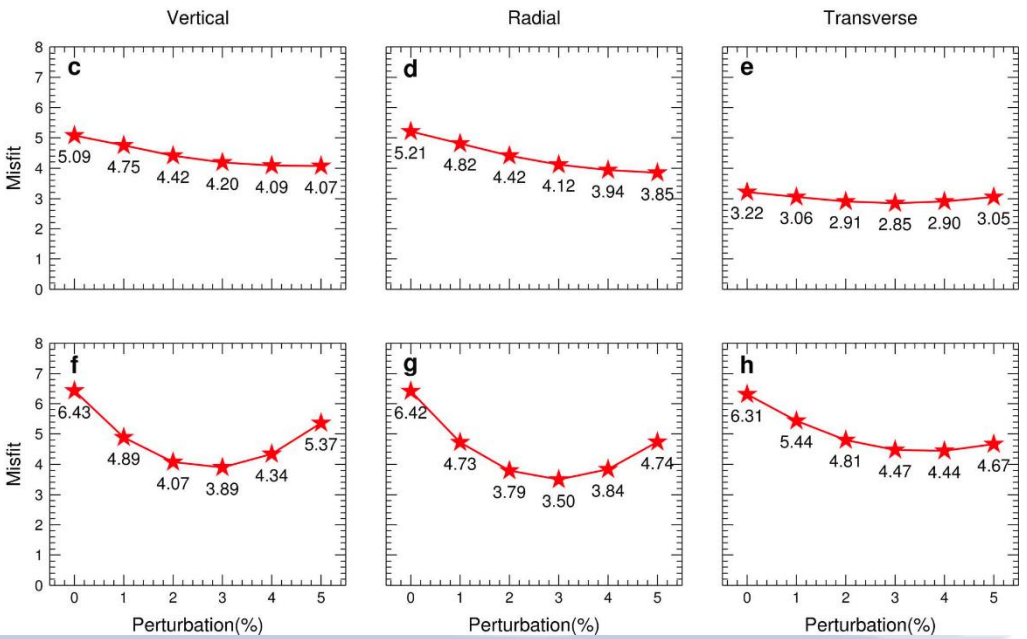

Flow chart

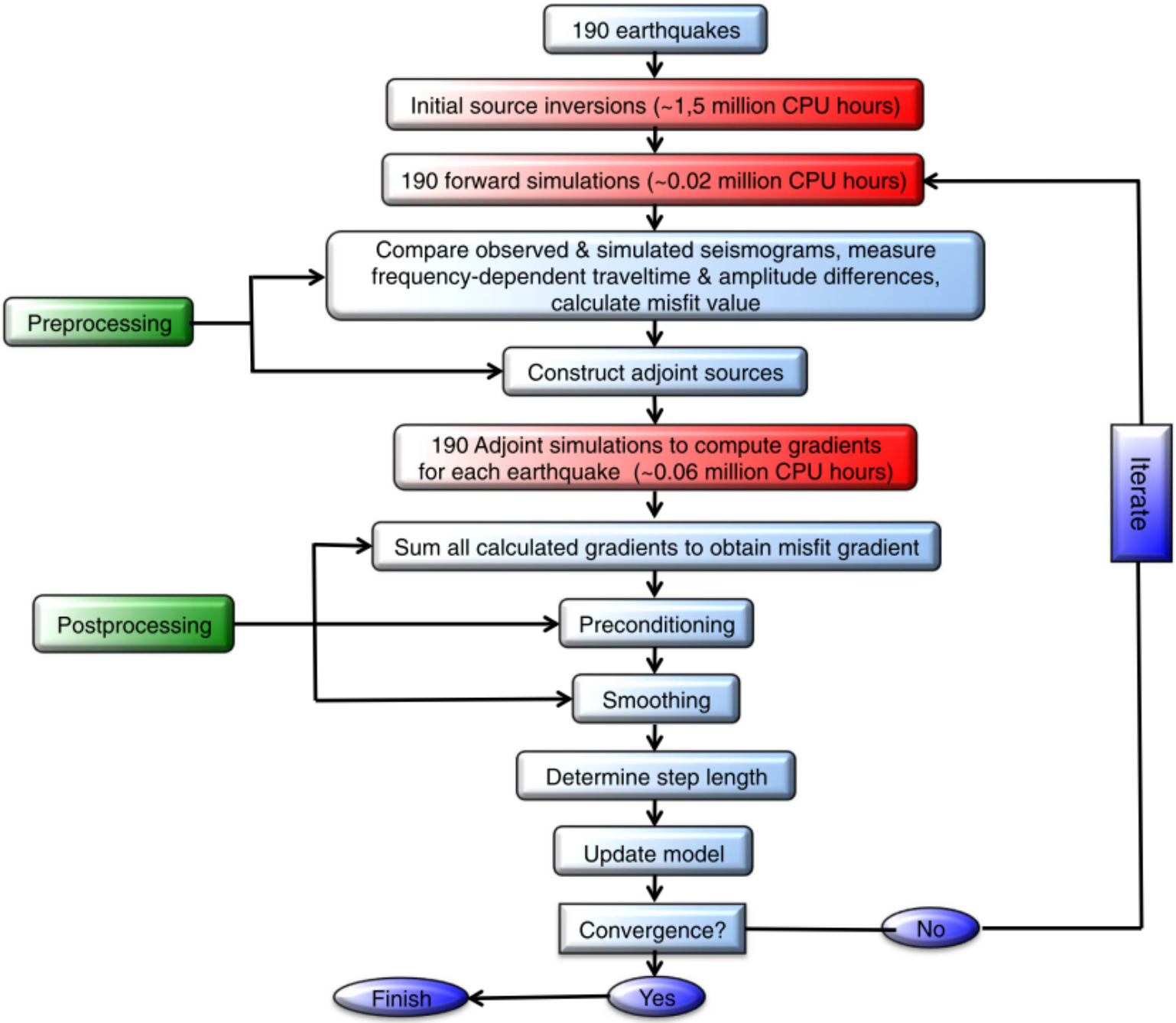
190 earthquakes
Initial source inversions (~1,5 million CPU hours)
190 forward simulations (~0.02 million CPU hours)
Compare observed & simulated seismograms, measure frequency-dependent traveltime & amplitude differences, calculate misfit value
Preprocessing
Construct adjoint sources
190 Adjoint simulations to compute gradients for each earthquake (~0.06 million CPU hours)
Sum all calculated gradients to obtain misfit gradient
Postprocessing
Preconditioning
Smoothing
Determine step length
Update model
Convergence?
No
Iterate
Finish
Yes

Stage 2: inversion steps

Stage 2: Misfit function including both phase and amplitude

$$\chi_{\mathrm{II}} = w_\phi\, \chi^\phi + w_A\, \chi^A$$

$$\chi^\phi = \sum_{c=1}^{N_c} w_c \sum_{m=1}^{N_m} \int w_m \left[\frac{\Delta\tau_m(\omega)}{\sigma_m^\phi(\omega)}\right]^2 \mathrm{d}\omega,$$

$$\chi^A = \sum_{c=1}^{N_c} w_c \sum_{m=1}^{N_m} \int w_m \left[\frac{\Delta \ln A_m(\omega)}{\sigma_m^A(\omega)}\right]^2 \mathrm{d}\omega,$$

Sensitivity kernels

Inverse Shear quality factor

$$\delta\chi_{\mathrm{II}} = \int_V \mathrm{K}_c\, \delta\ln c + \mathrm{K}_{\beta_\mathrm{v}}\, \delta\ln\beta_\mathrm{v} + \mathrm{K}_{\beta_\mathrm{h}}\, \delta\ln\beta_\mathrm{h} + \mathrm{K}_\eta\, \delta\ln\eta + \mathrm{K}_{Q^{-1}}\, \delta Q^{-1}\, \mathrm{d}V,$$

$$\mathrm{K}_{Q^{-1}} = -\int_0^T 2\mu\, \mathbf{D}^\dagger(T-t) : \mathbf{D}(t)\, \mathrm{d}t,$$

$$\tilde{f}_i^\dagger(t) = \frac{1}{2\pi} \int_{-\infty}^{+\infty} [(2/\pi \ln(|\omega|/\omega_0 - i\,\mathrm{sgn}(\omega)]^*\, f_i^\dagger(\omega) \exp(i\omega t)\, \mathrm{d}\omega$$

Separate simulations for elastic and anelastic kernels

Stage 3: inversion steps

Stage 3: misfit function including both phase and amplitude (surface wave only)

$$\chi_{\mathrm{III}} = w_\phi \chi^\phi + w_A \chi^A,$$

In weakly anisotropic medium,

$$c(\omega,\theta) = c_0(\omega) + c_1(\omega)\cos(2\theta) + c_2(\omega)\sin(2\theta) + c_3(\omega)\cos(4\theta) + c_4(\omega)\sin(4\theta)$$

C_0: radially anisotropy
C_1,2: related to G, H, B_{s,c}
C_3,4: related to E_{s,c}
Total 13 parameters (5+8)

Select to invert for only radial anisotropy (L,N) and azimuthal anisotropy (G_c, G_s)

$$\delta\chi_{\mathrm{III}} = \int_V \mathrm{K}_L \delta L + \mathrm{K}_N \delta N + \mathrm{K}_{G_c} \delta G_c + \mathrm{K}_{G_s} \delta G_s \, \mathrm{d}V,$$

$$= \int_V \mathrm{K}_{\beta_\mathrm{v}} \delta \ln\beta_\mathrm{v} + \mathrm{K}_{\beta_\mathrm{h}} \delta \ln\beta_\mathrm{h} + \mathrm{K}_{G_c'} \delta G_c' + \mathrm{K}_{G_s'} \delta G_s' \, \mathrm{d}V,$$

Fast axis & Strength:

$$G_0 = \sqrt{G_s^2 + G_c^2},$$

$$\zeta = \frac{1}{2}\arctan(G_s/G_c).$$

Misfit Reduction

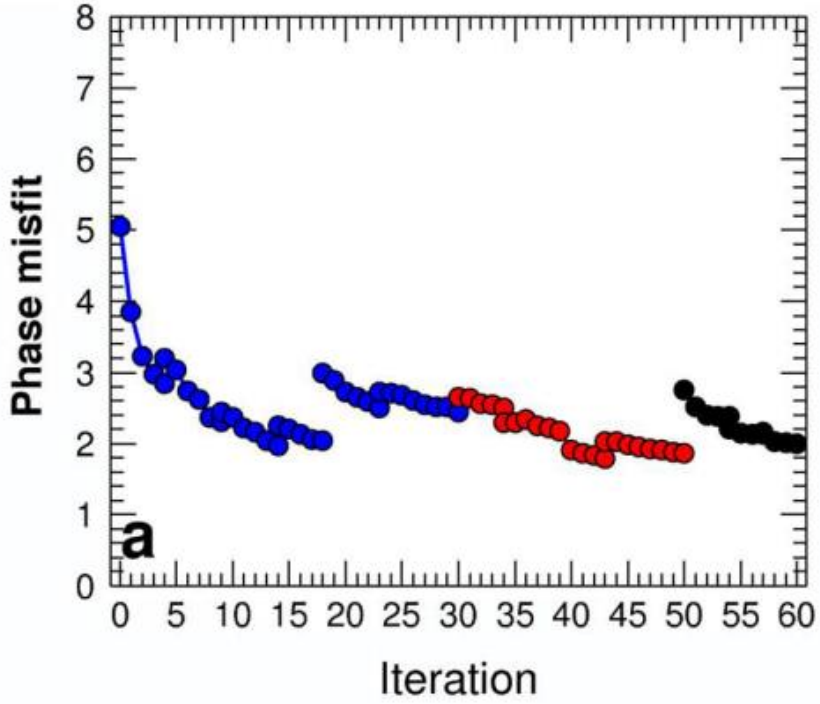

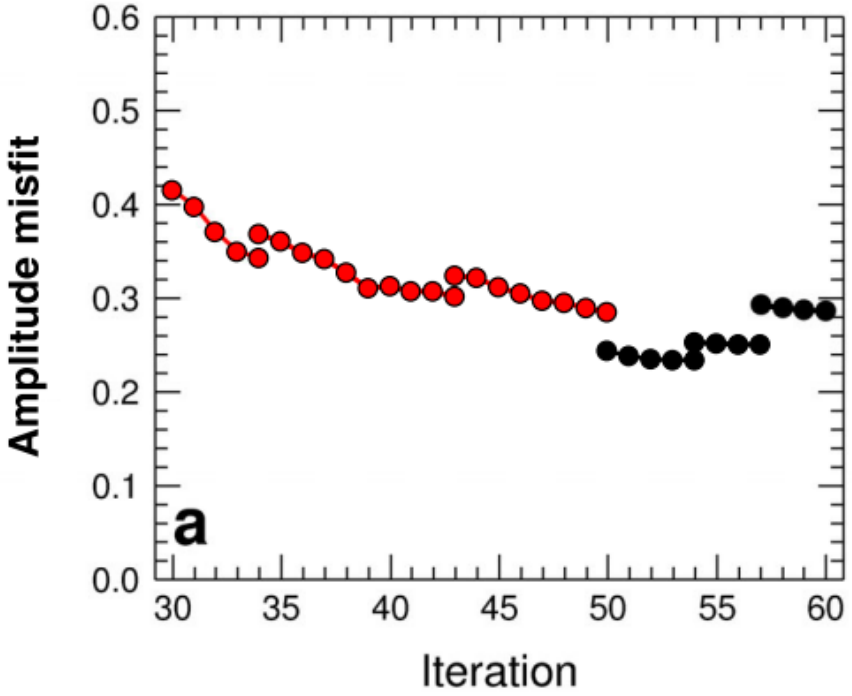

Traveltime anomaly Histogram

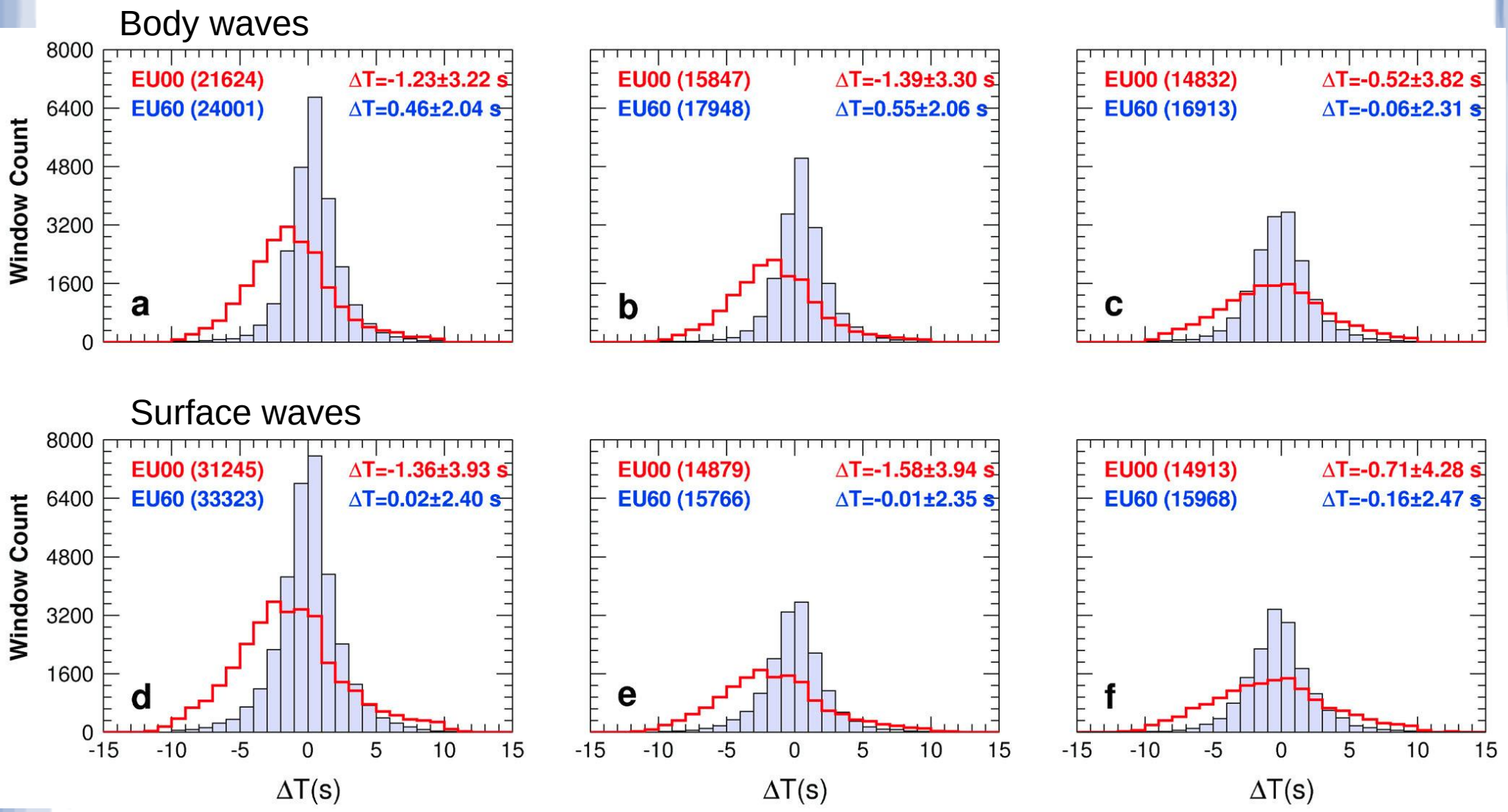

Final Images

Vs

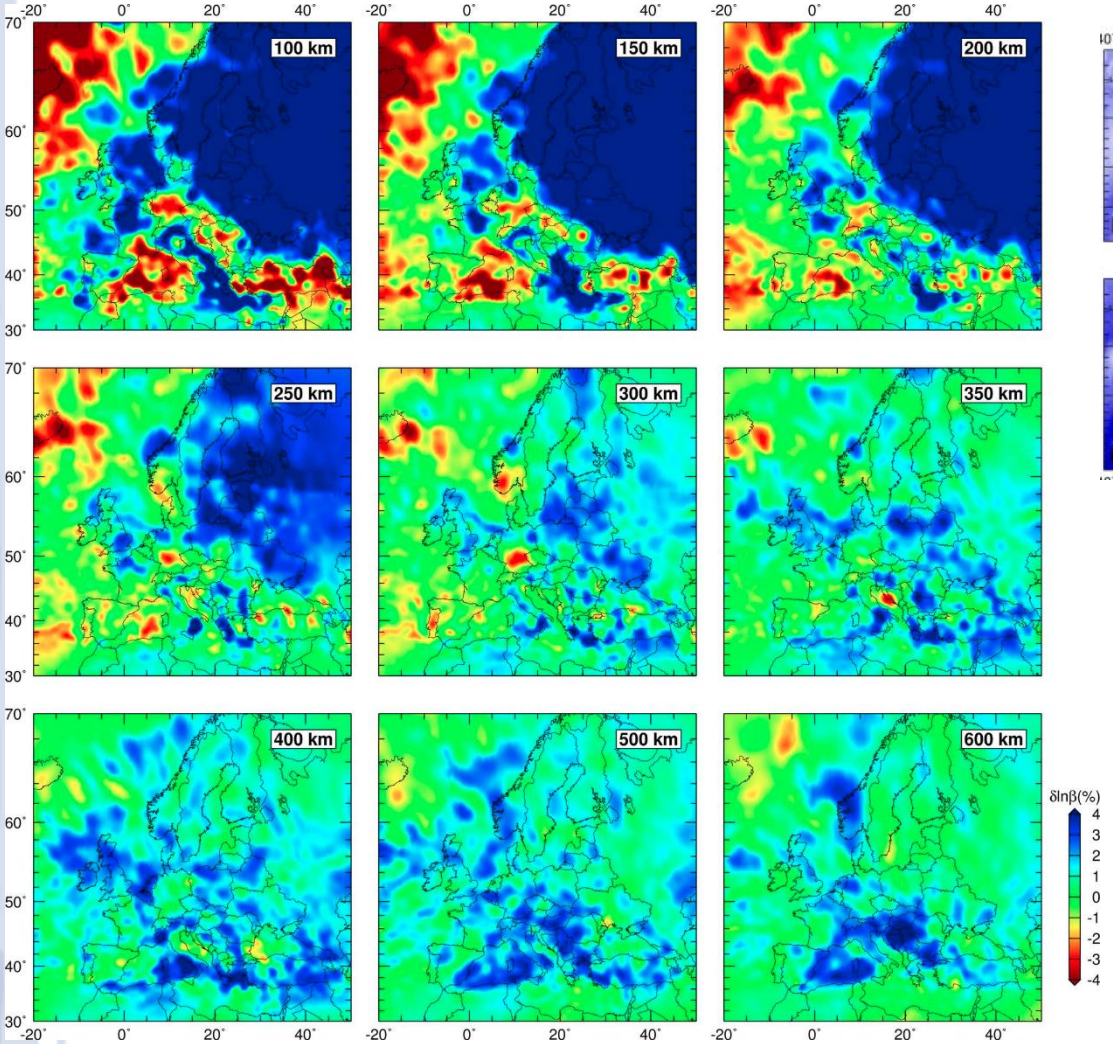

xi

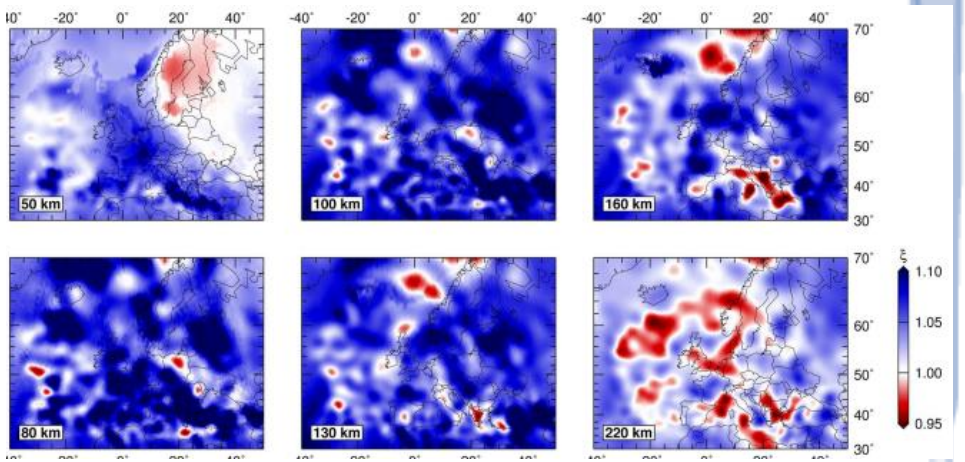

Final images

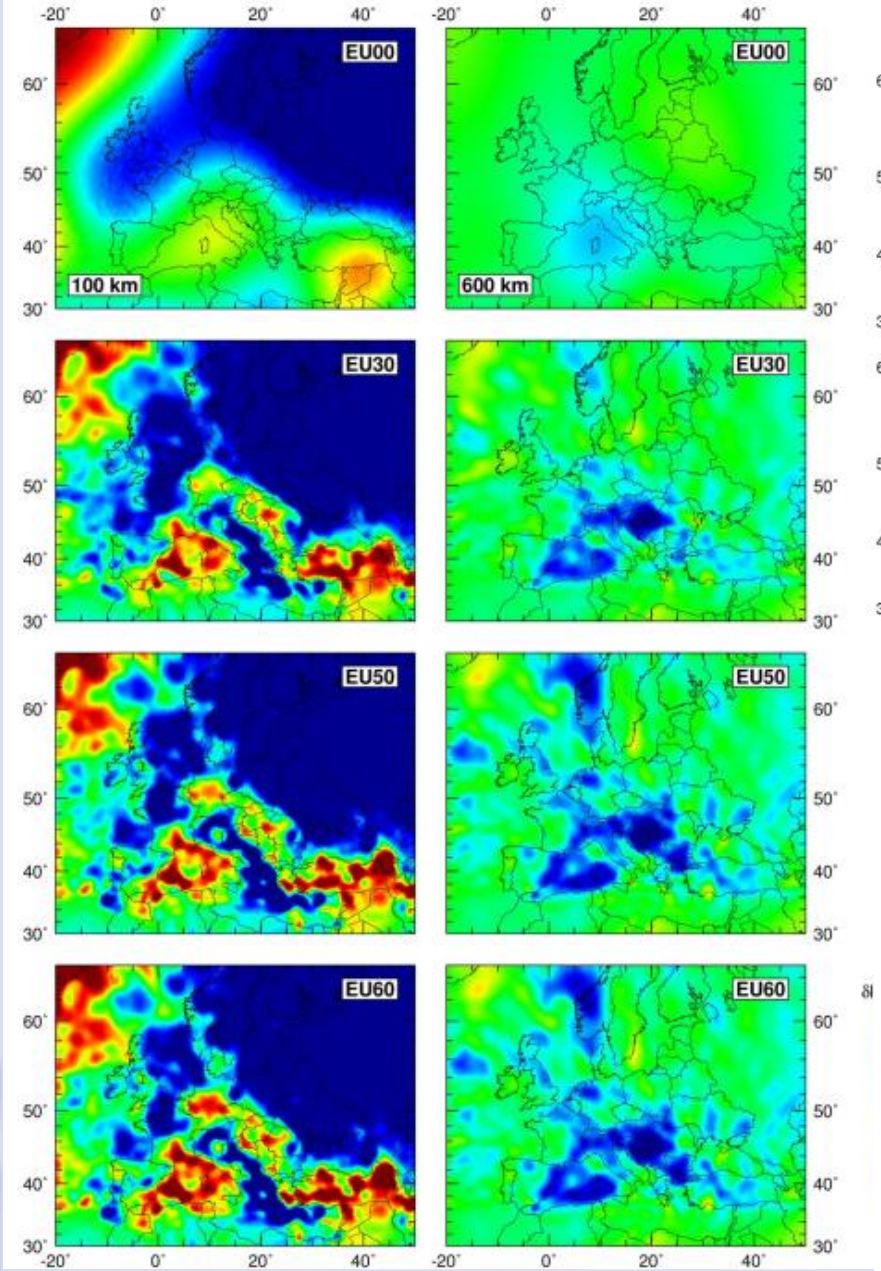

Vs comparison at 100 km

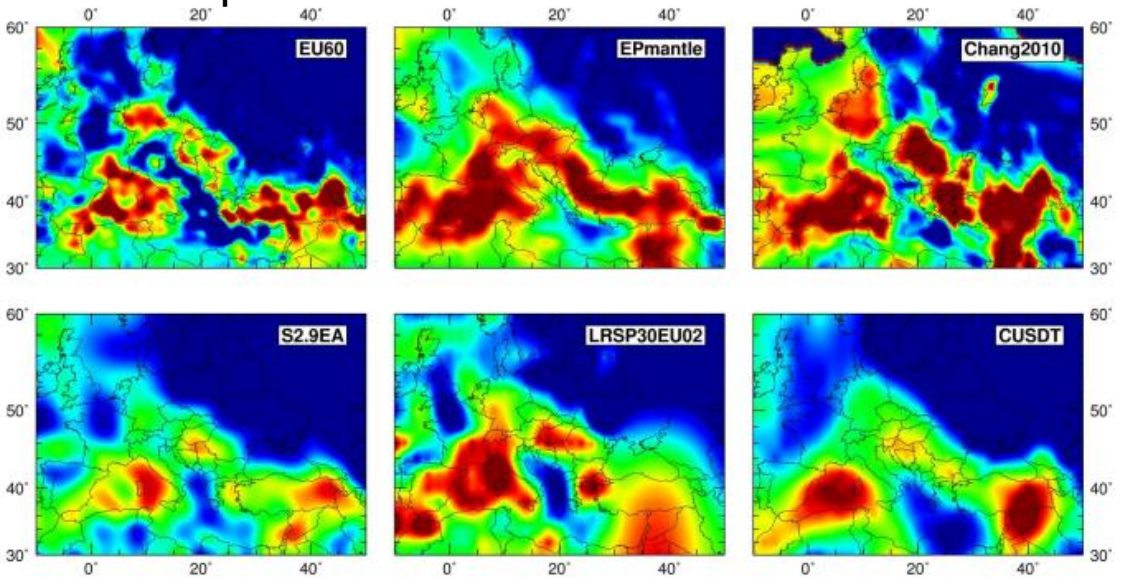

Xi at 100 km

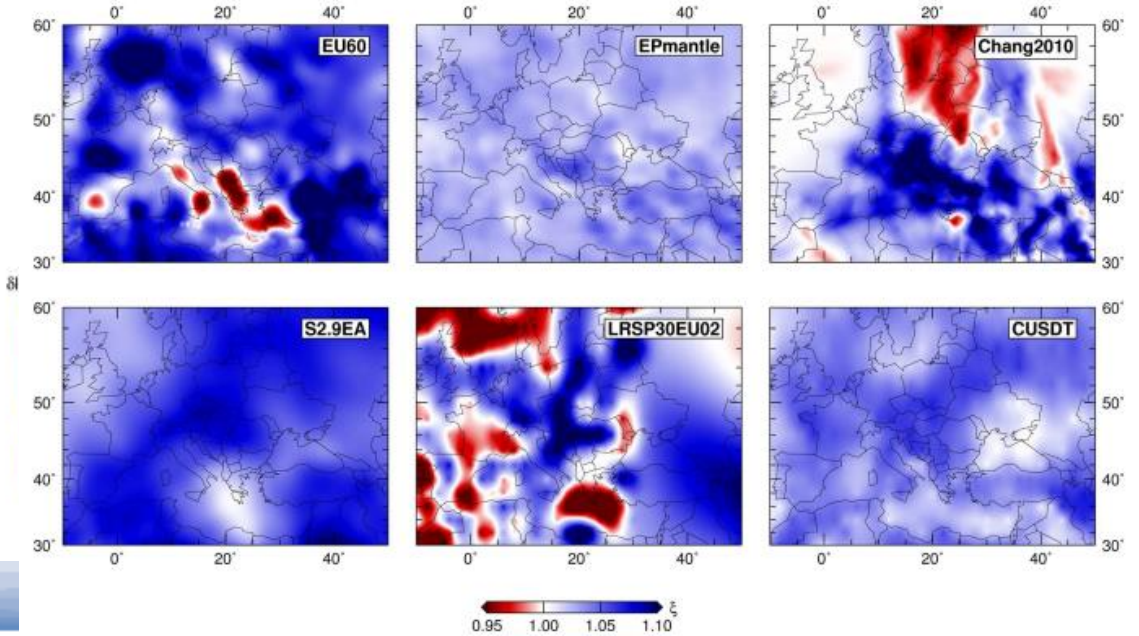

EU60: depth cross-sections

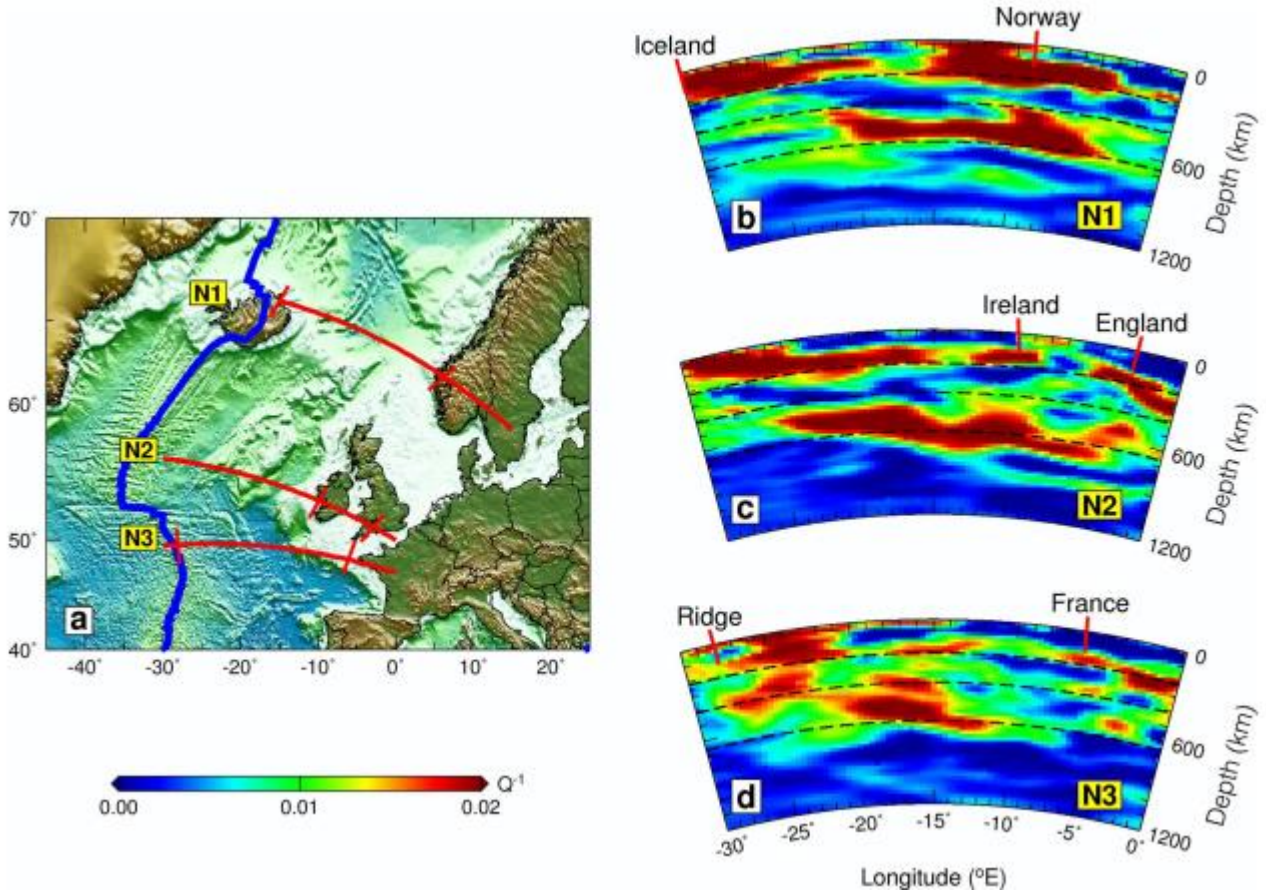

EU60: azimuthal anisotropy

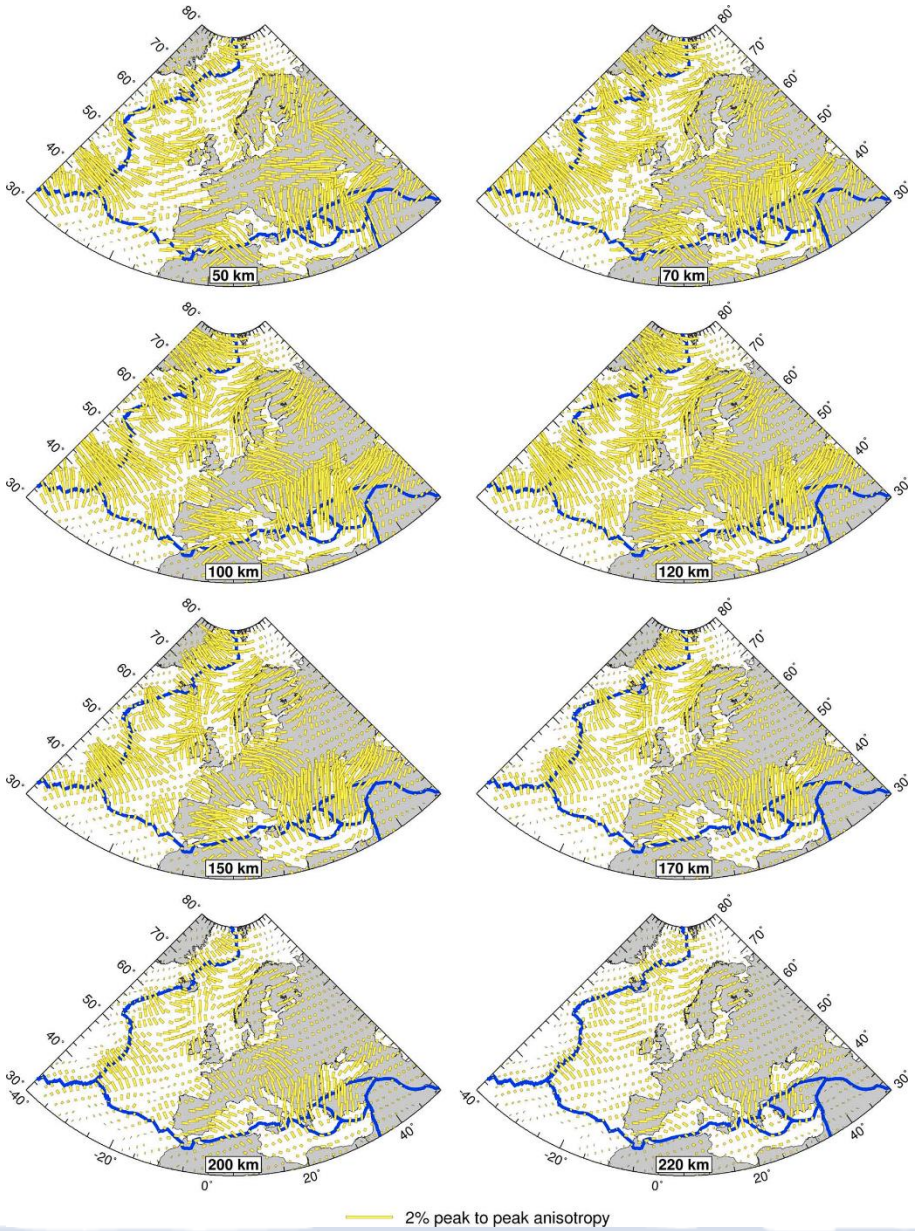

Resolution test: point spread functions

Stage 1: point spread function, Vsh, Vsv

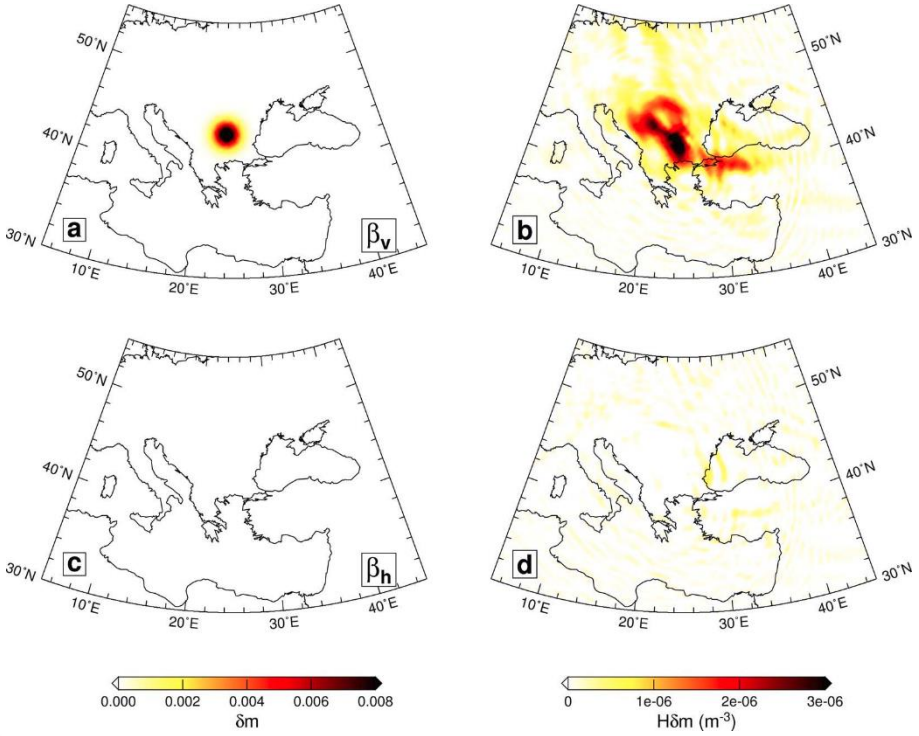

Stage 2: Vsh, Vsv, 1/Q

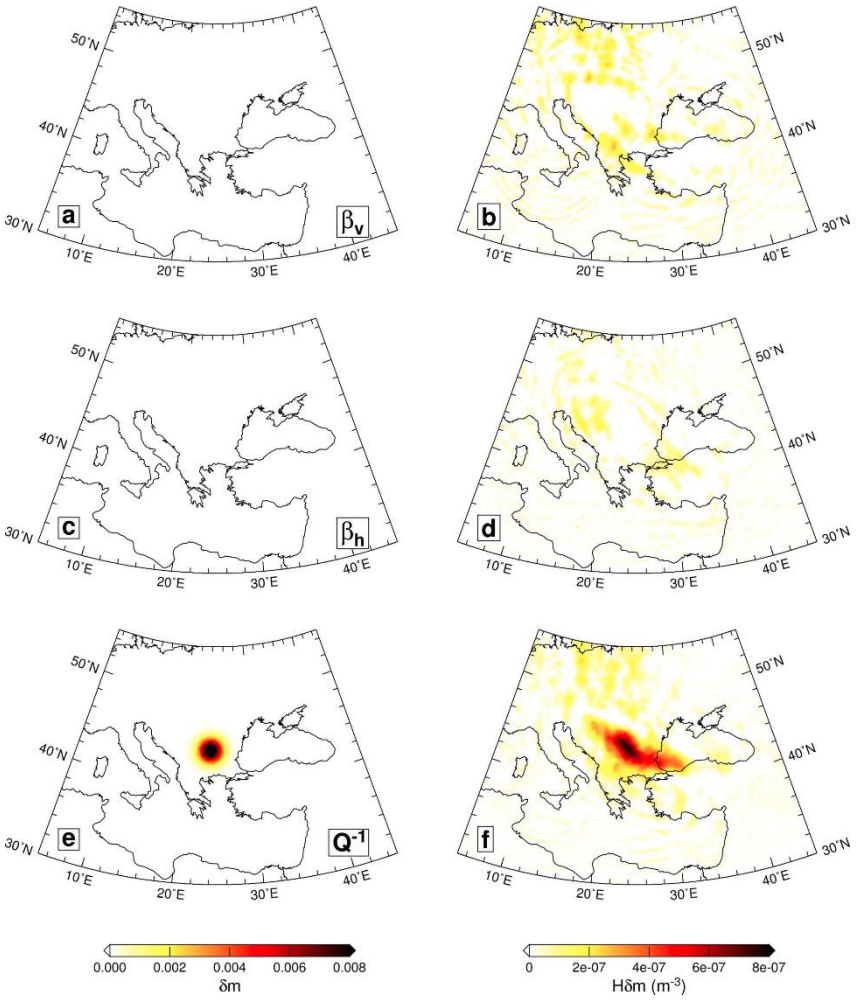

Point spread function (cont)

Stage 3:
L, N, Gc, Gs

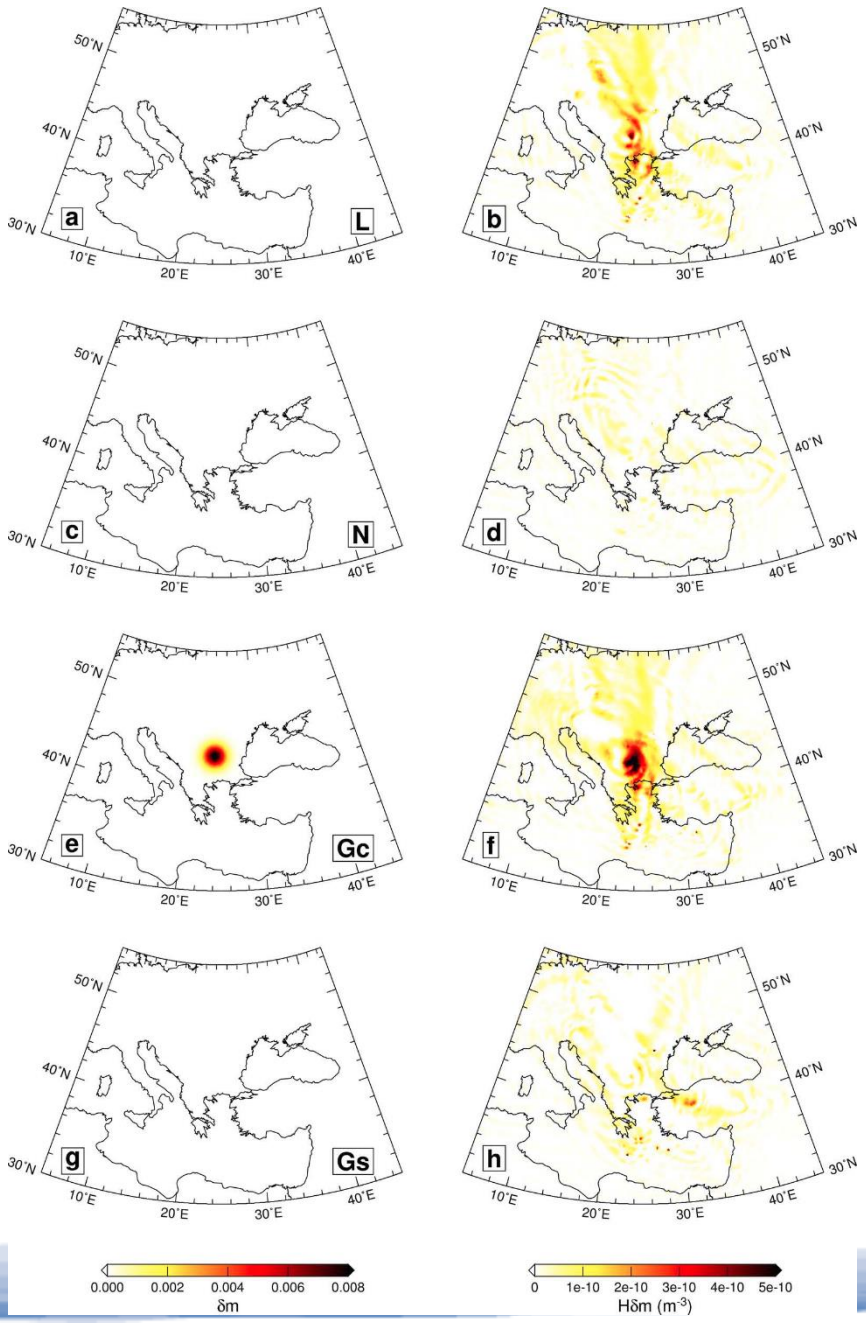

Coverage: Approximate Hessian Diagonal

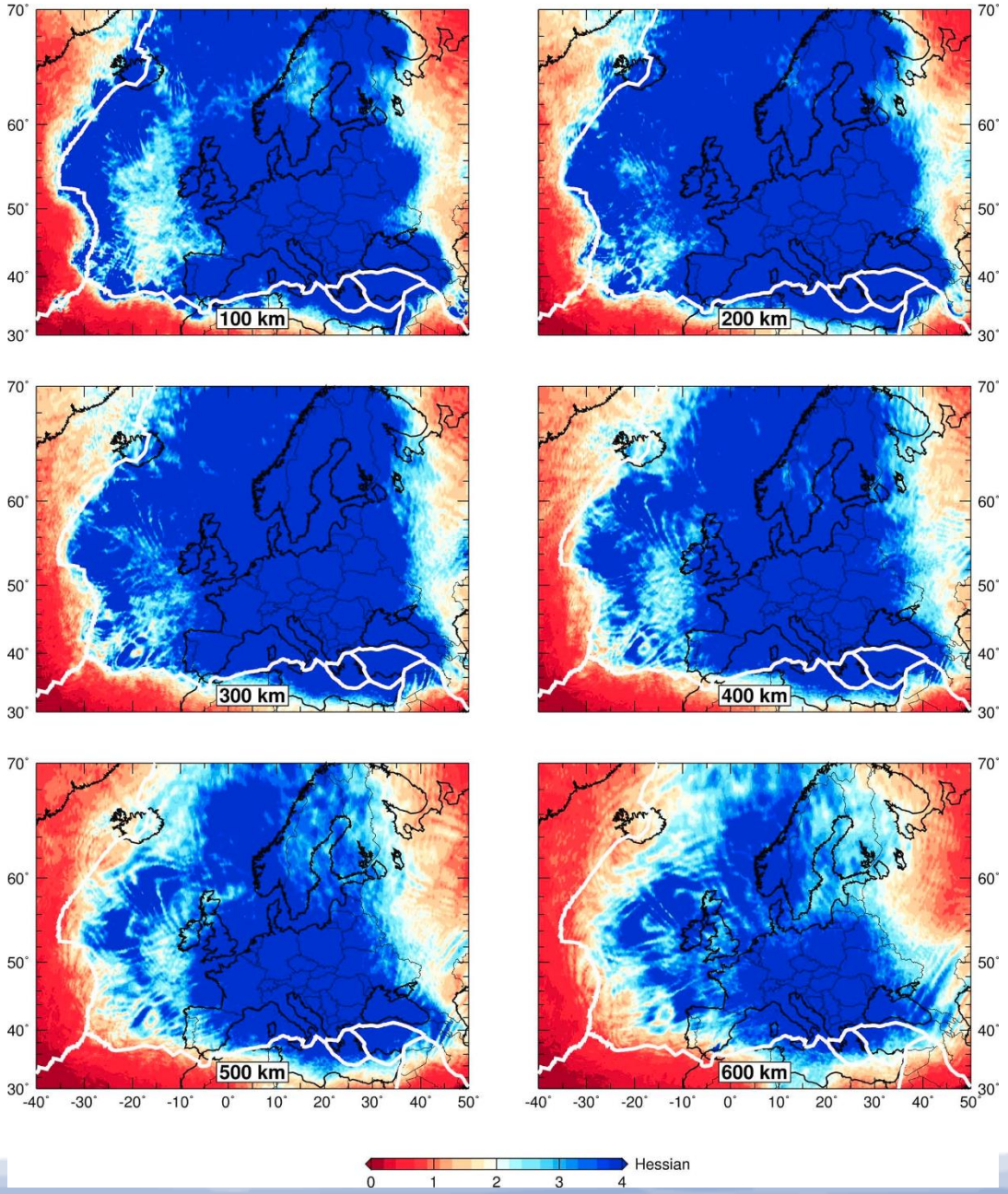

Adjoint tomography of East Asia

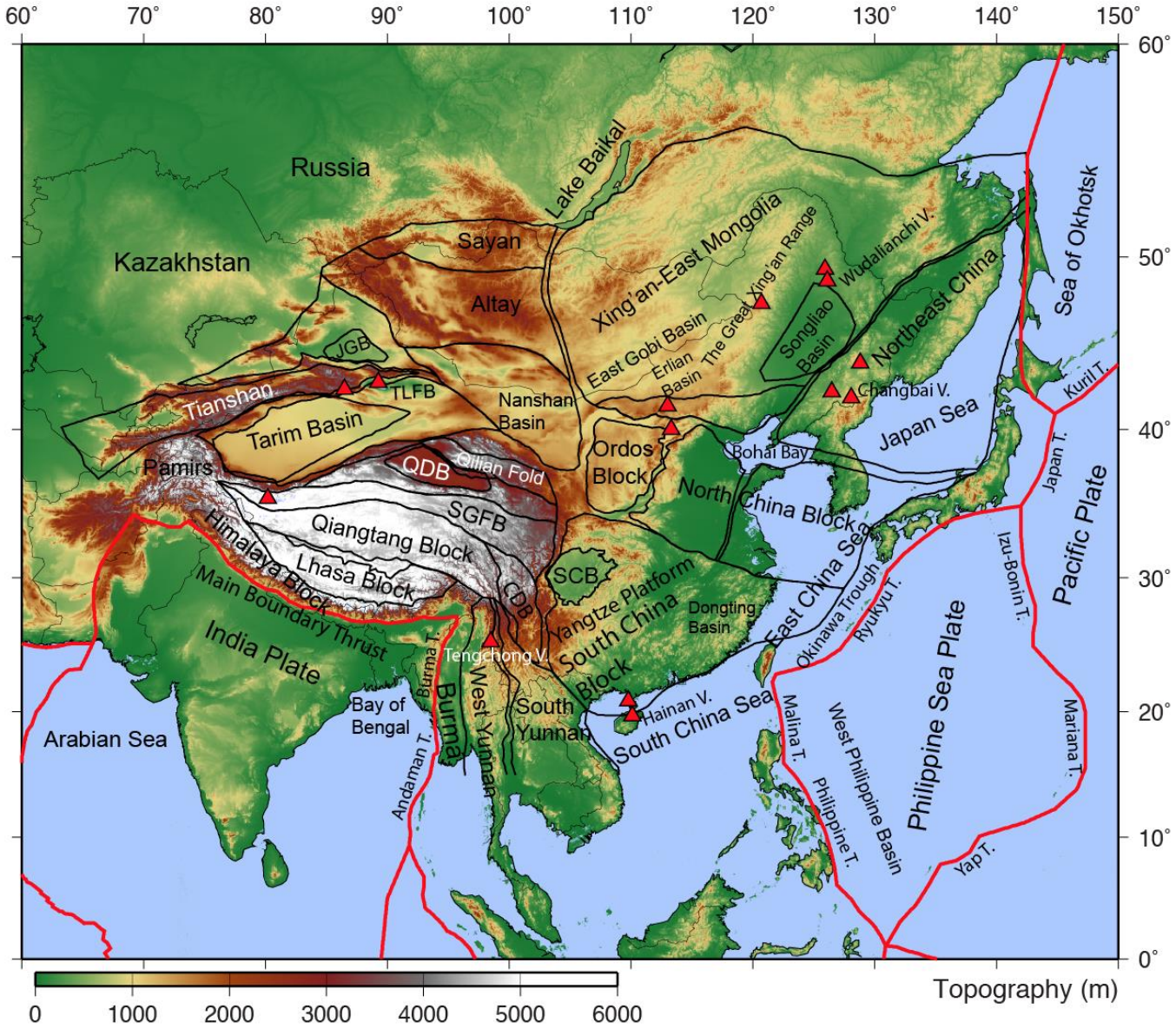

* continental-continental collision
* subduction
* basin formation
* intracontinental rift
Intraplate volcanism

* large variation in topography

* inversion of both body and surface waves for 3D radially anisotropic models of both the crust and mantle

* eliminates crustal corrections

Chen et al (2015a,b)

Dataset

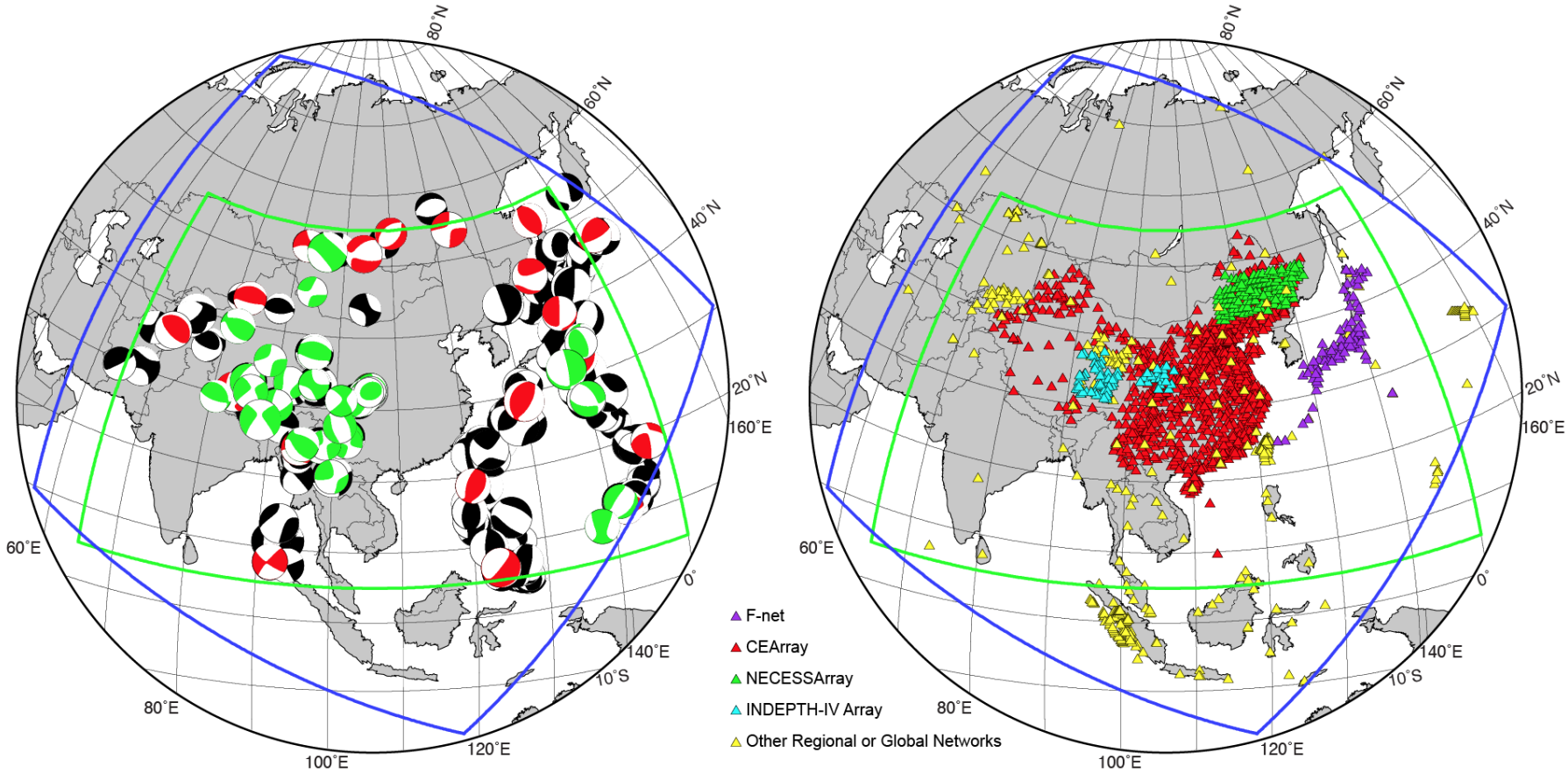

* 227 earthquakes (Mw=5-7, red: 20 subset; green: 39 extra)
* 1869 stations (majority are broadband stations) from F_net, CEArray, NECESSArray, INDEPT IV array
* 1.7 million frequency-dependent traveltime measurements from body and surface waves

Adjoint tomography Procedures

* 3D initial model: S362ANI (Kustowski et al 2008) + CRUST 2.0 (Bassin et al 2000)

* forward modelling based on SPECFEM3D_GLOBE package (E-topo2, Moho, 410,660 topography, 8km/5km h/v grid spacing in the crust, accurate up to 10 sec)

* Updating CMT source parameters (CMT3D, Liu et al 2004): reinverted based on 3D initial model and seisograms filtered at 30-60 s (body), 50-100 s (surf.), and 80-150 s (surf) → depth mostly becomes shallow (computational very costly, eqv. 15 structural iterations, only done once)

* frequency-dependent measurements between data and 3D synthetics made at automatically picked windows: FLEXWIN (Maggi et al 2009) for three passbands 15s-40s (body-wave-only), 30-60s, and 50-100 s for the first 12 iteration, and the lower bound is lowered to 12, 20 and 40 s.

* total ~ 1.2 M measurements for the initial model, and 1.7M measurements for the final model

Windowing

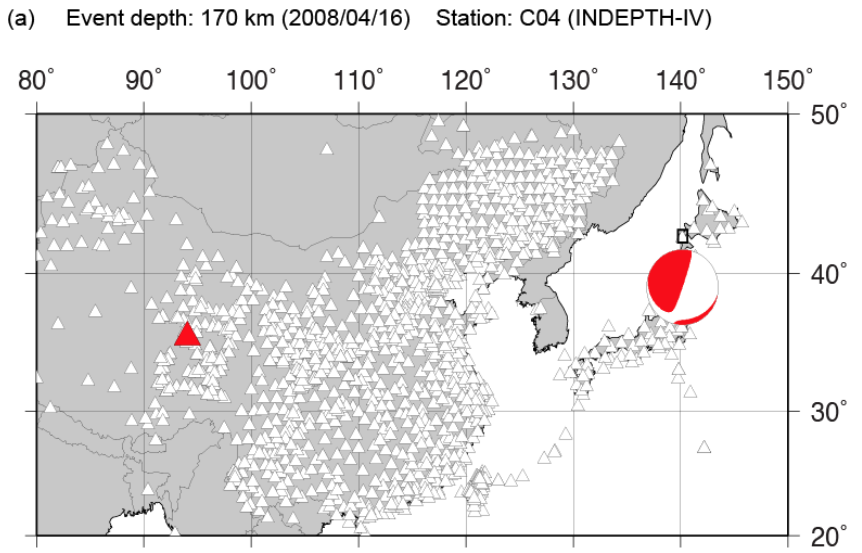
(a) Event depth: 170 km (2008/04/16) Station: C04 (INDEPTH-IV)
80˚ 90˚ 100˚ 110˚ 120˚ 130˚ 140˚ 150˚
50˚ 40˚ 30˚ 20˚

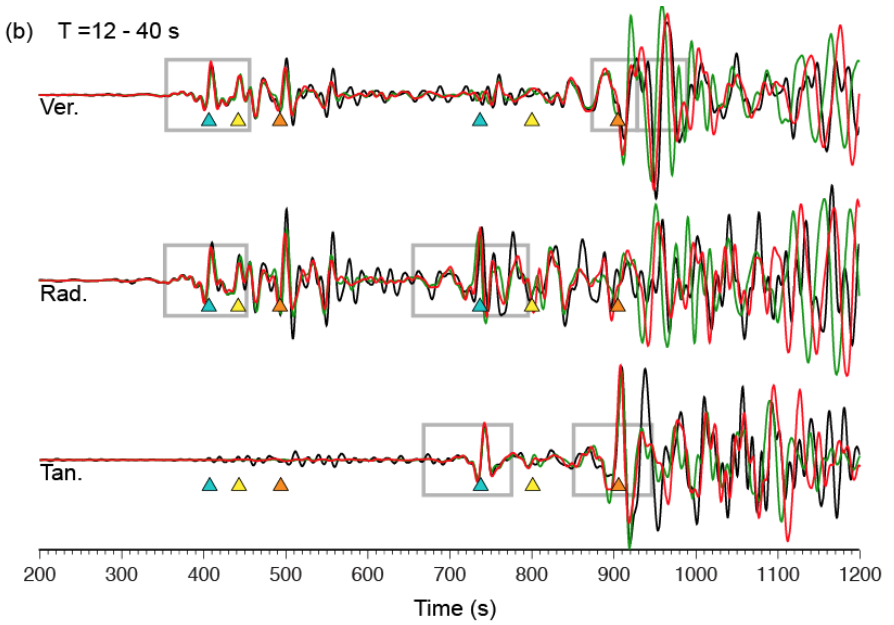
(b) T =12 - 40 s
Ver.
Rad.
Tan.
200 300 400 500 600 700 800 900 1000 1100 1200
Time (s)

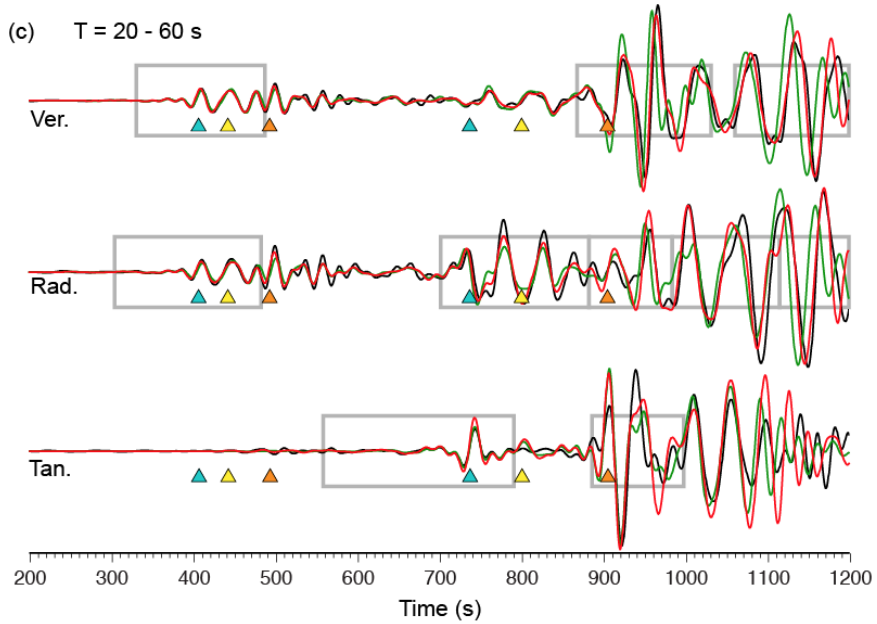
(c) T = 20 - 60 s
Ver.
Rad.
Tan.
200 300 400 500 600 700 800 900 1000 1100 1200
Time (s)

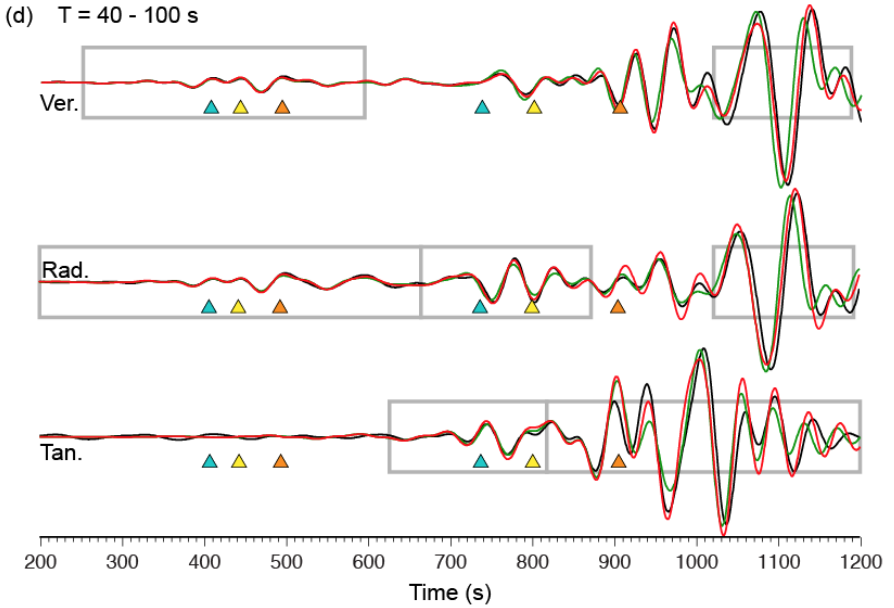
(d) T = 40 - 100 s
Ver.
Rad.
Tan.
200 300 400 500 600 700 800 900 1000 1100 1200
Time (s)

Adjoint tomography Procedures

* Define misfit function $\phi = \frac{1}{N_c}\sum_c \phi_c, \quad \phi_c = \sum_{pc}\int \left(\frac{\Delta T_{pc}(\omega)}{\sigma_{pc}(\omega)}\right)^2 d\omega$

* Parameterization in terms of Vc, Vsh, Vsv and eta (dln(rho) = 0.33dln(Vs)):

$$\delta T = \int_V \left(K_{V_c}\delta \ln V_c + K_{V_{SH}}\delta \ln V_{SH} + K_{V_{SV}}\delta \ln V_{SV} + K_\eta \delta \ln \eta\right) dV$$

* adjoint sources are computed by assimilating measures

* Event sensitivity kernels are computed by the adjoint methods: interaction of forward and adjoint wavefields), and then summed to obtain gradient vector $\frac{\partial \phi}{\partial m}$

* Apply approximate diagonal of Hessian matrix as preconditioner and smoothed with 5km (v)/ 100-60 km (h) Guassian function

* optimal model in the gradient direction is obtained through line search: step length determined by a subset of 20 events

* model is updated based on gradient vector and step length,

* Next iteration

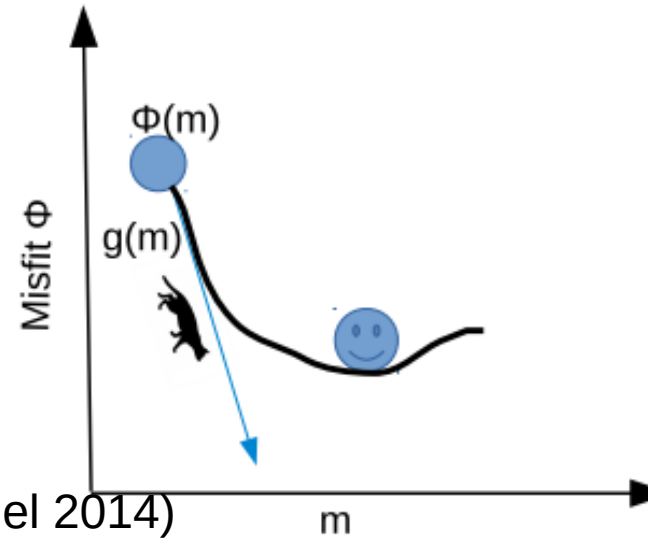

Total 20 iterations (8 million CPU)
Final model: EARA2014 (East Asia Radially Anisotropic Model 2014)

Line Search & Misfit reduction

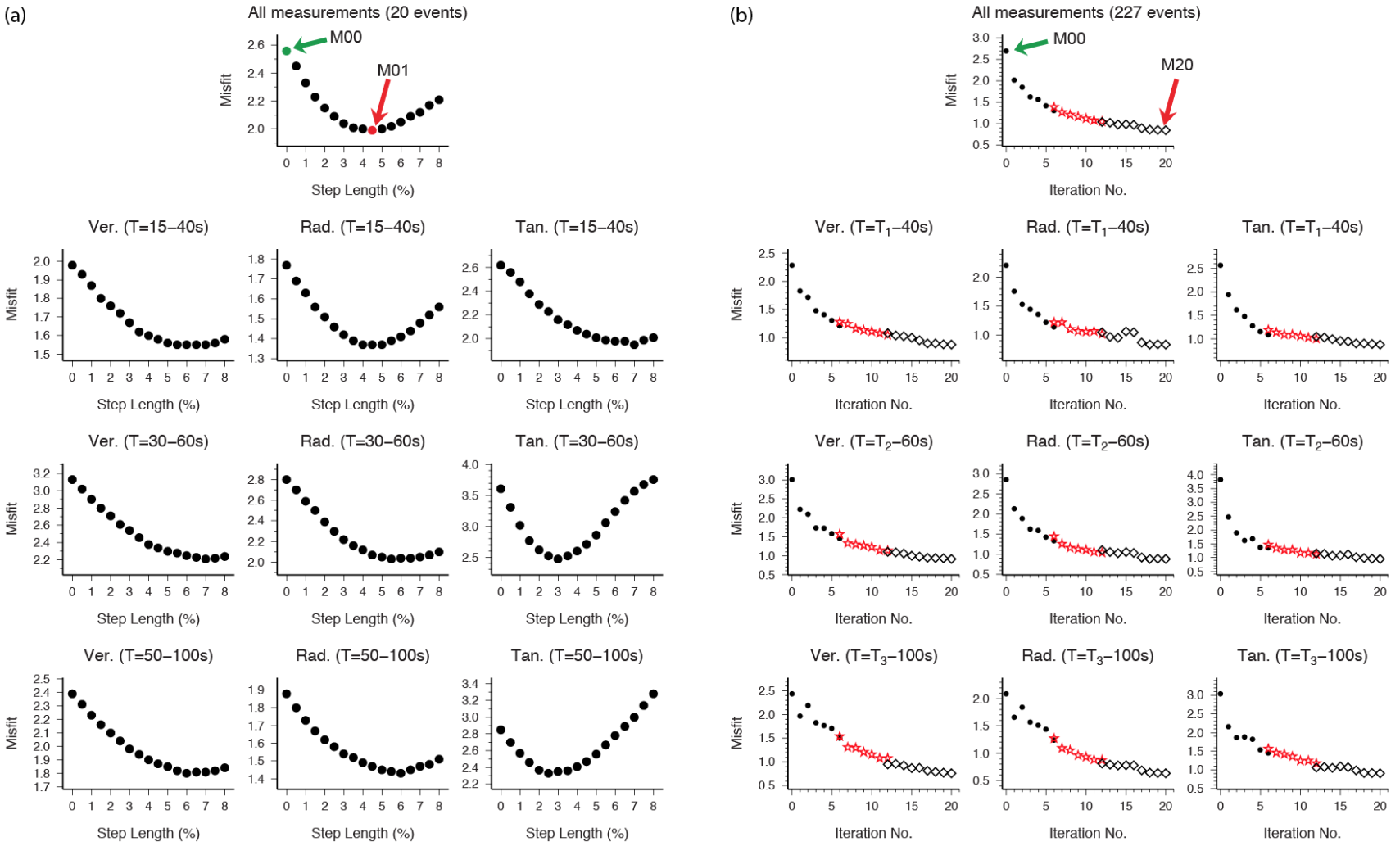

Model Quality Assessment

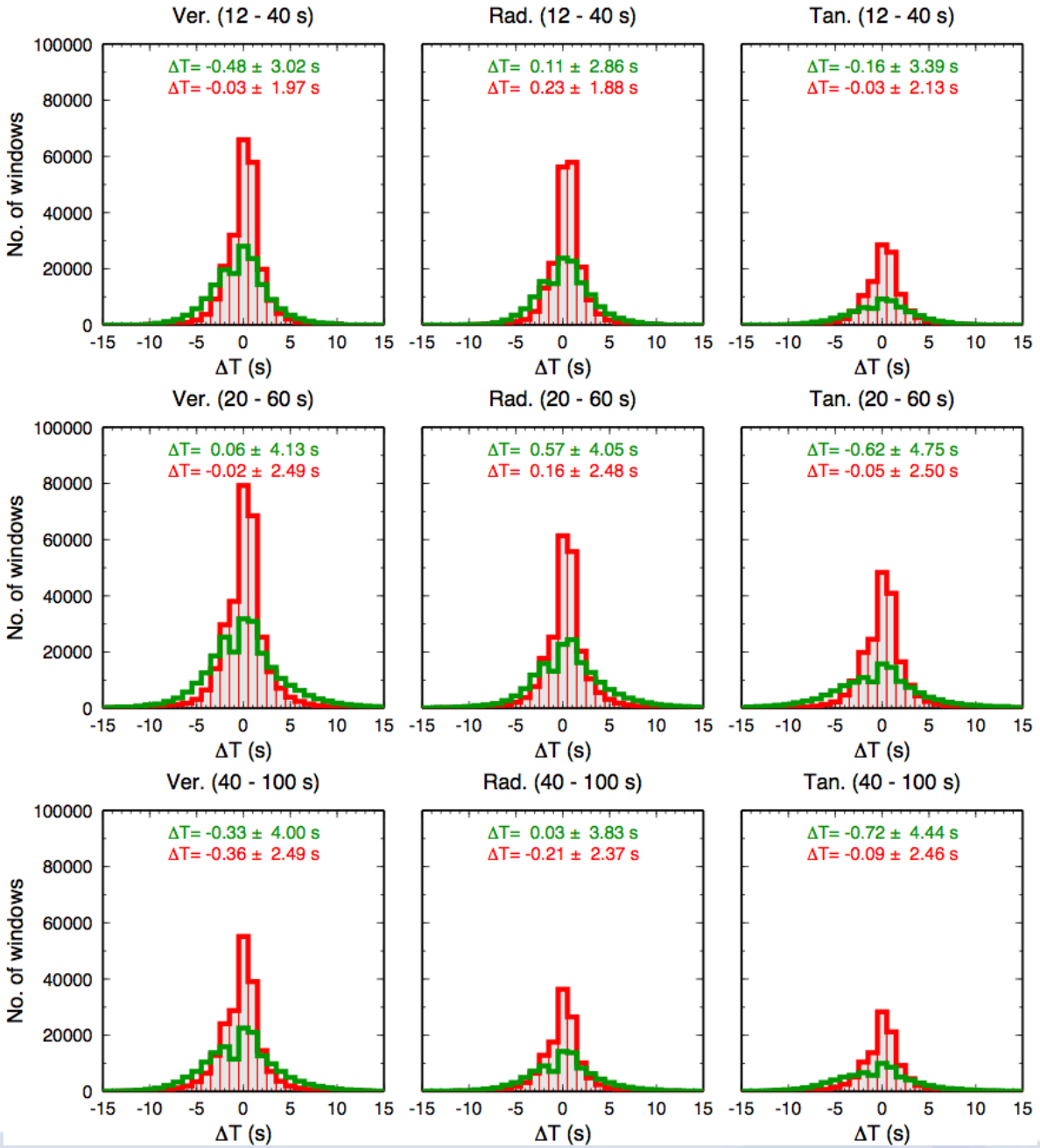

Mean/std of measurements:

Initial model: -0.12+/-3.88 s
Final model: -0.03+/-2.32 s

39 extra earthquakes:
Initial model: -0.10+/-4.24 s
Final model: -0.24+/-3.11 s

Vsv Model updates

S362ani Global model

Final Vsv model

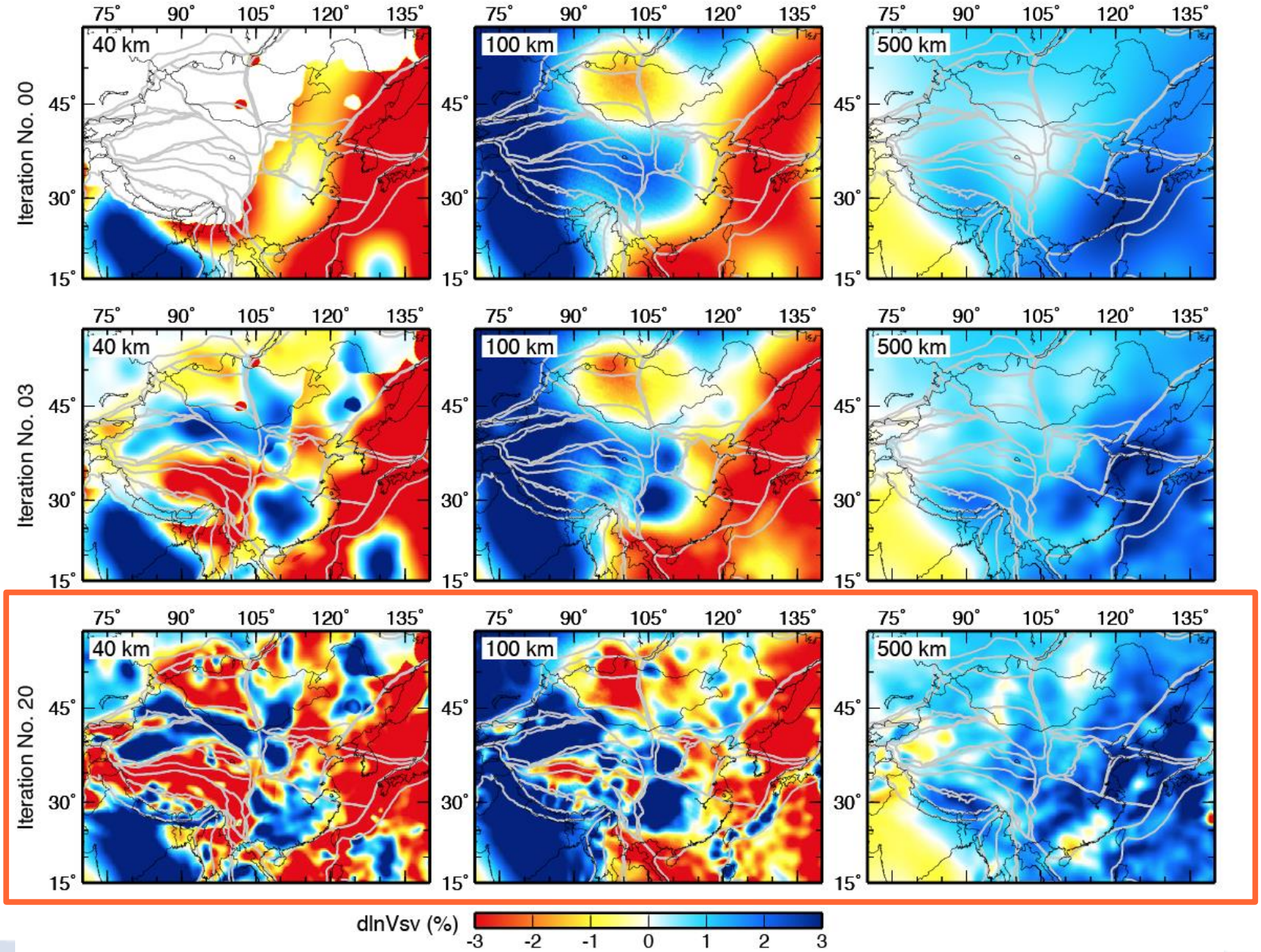

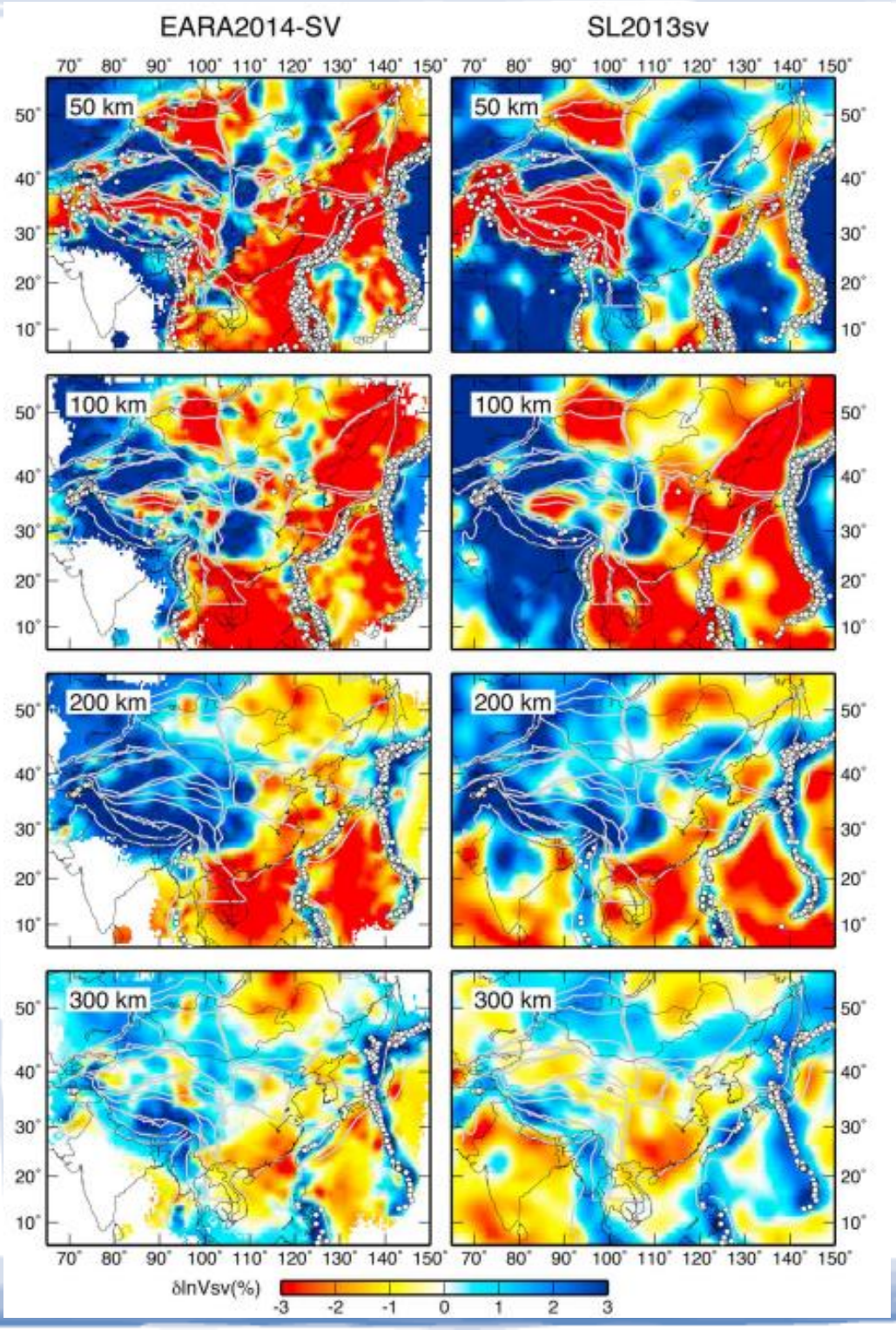

Vsv model comparison

With high-resolution global shear velocity model SL2013sv from Schaeffer & Lebedev (2013)

Similarities:
* 50-100 km: low V beneath Tibetan plateau and Altay-Sayan Mnt range
* 200 km: high-V beneath central/southern Tibet down to TZ
* 50-200 km, high V beneath Ordos and Yangtze platform

A more refined model:
* narrow slabs from 200-400km at Pacific margin
* confined low V to Qiangtang and Songpan Ganzi blocks

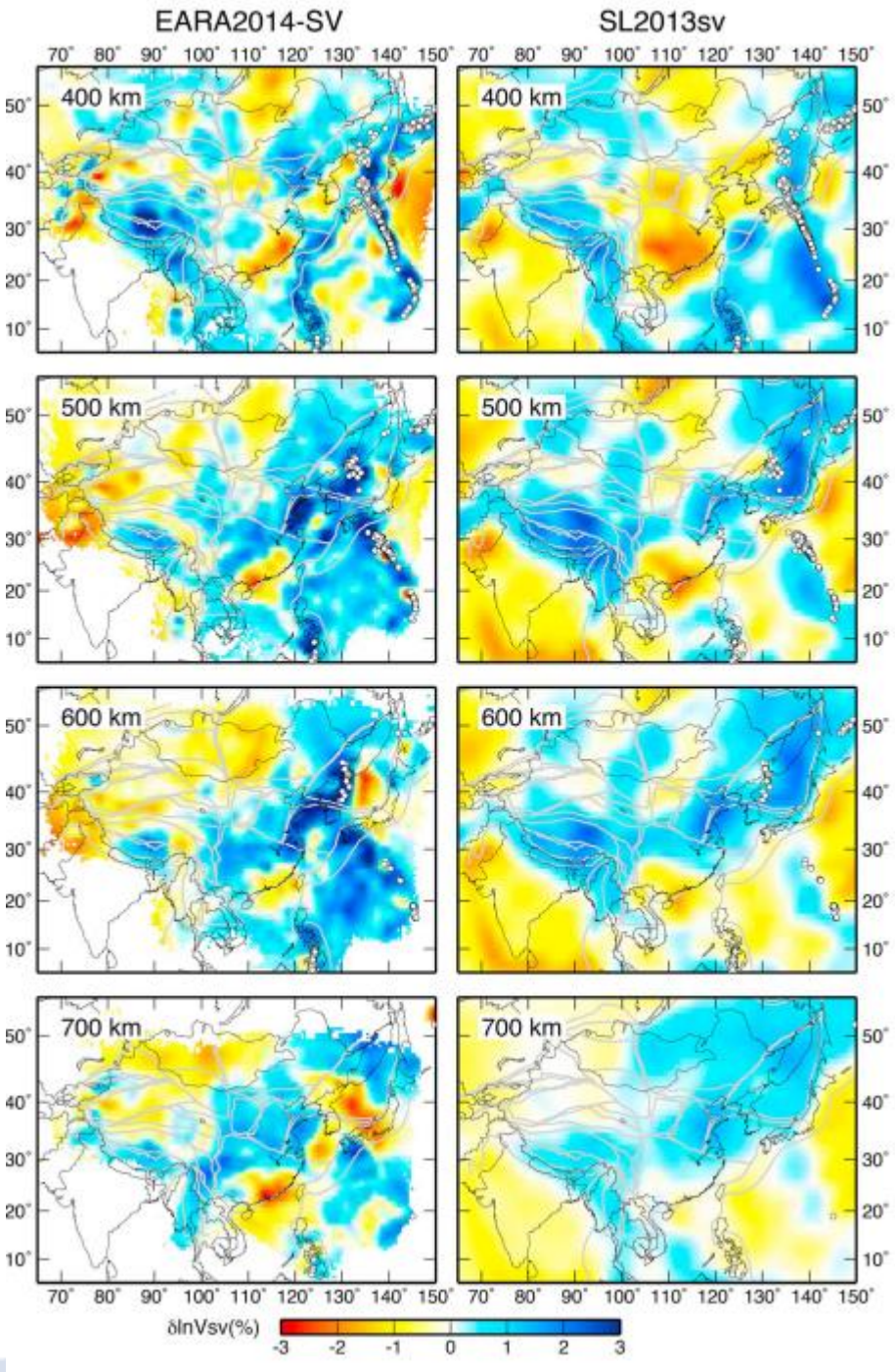

Vsv model comparison

With high-resolution global shear velocity model SL2013sv from Schaeffer & Lebedev (2013)

Between 400 – 700 km

* narrower slabs
* hainan plume

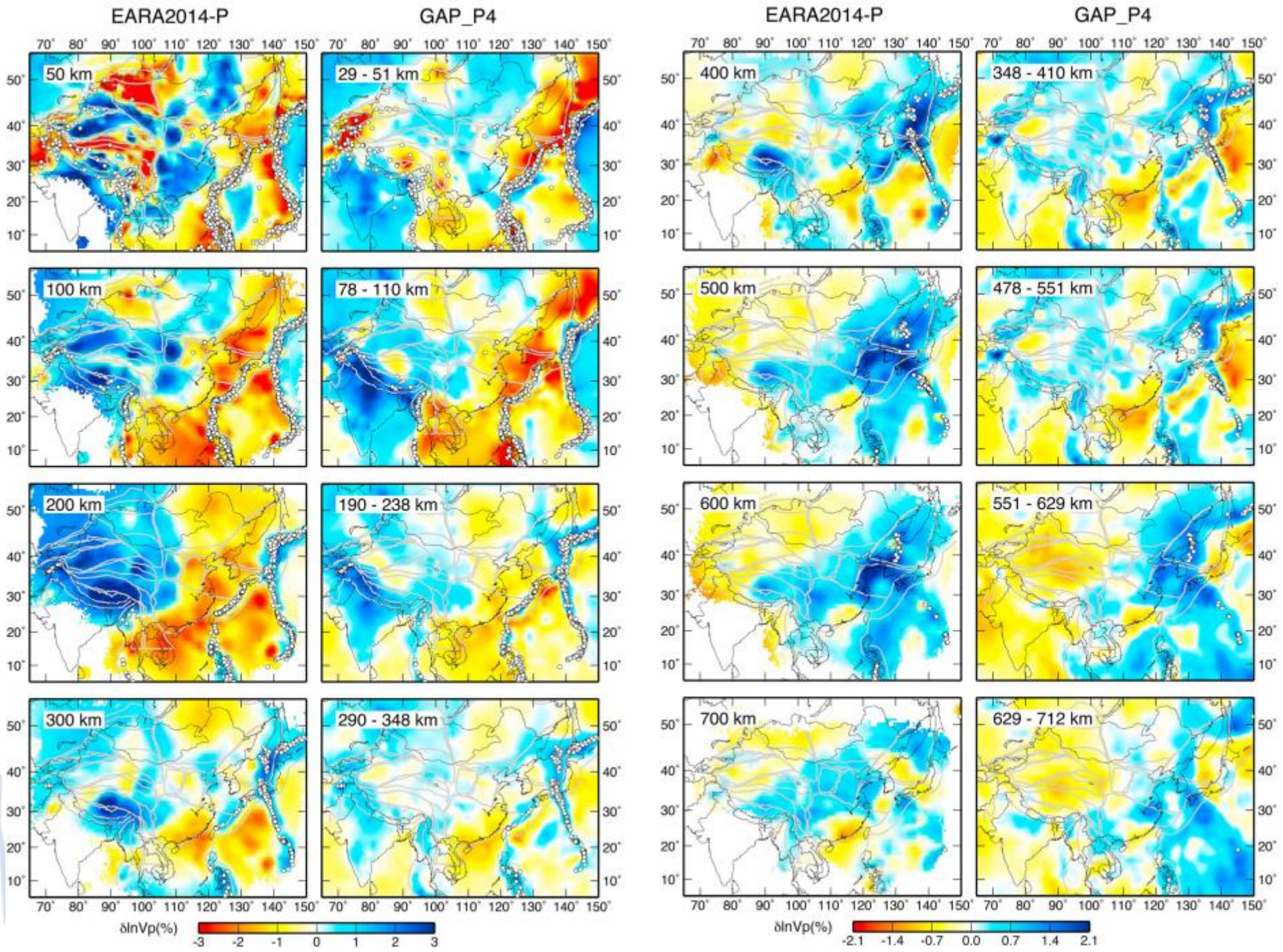

Voigt average Vp and Vp from GAP_P4 (Obayashi et al 2013)

Challenges

* Wave simulations are generally performed on HPC

* Data and synthetic processing for a large number of events and stations

* Preprocessing requires running a series of software packages sequentially (windowing, measurement, adjoint source calculation)

* Optimization strategies (step length, CG, BFGS, etc)

* monitoring waveform and traveltime fits at each iteration

* Many iterations …

→ community based effort to develop more general inversion frameworks that utilize Advanced Data Format, Scientific Workflow, etc

ObsPy: data acquisition and processing

obspy / **obspy** Watch

Code Issues 101 Pull requests 44 Wiki Pulse Graphs

Home

Tobias Megies edited this page 16 days ago · 157 revisions

ObsPy

A Python Framework for Seismology

ObsPy is an open-source project dedicated to provide a **Python framework for processing seismological** data. It provides parsers for common file formats, clients to access data centers and seismological signal processing routines which allow the manipulation of seismological time series.

The goal of the ObsPy project is to facilitate **rapid application development for seismology**.

Contents

- Acknowledging
- News
- Getting Started

Krischer et al 2015

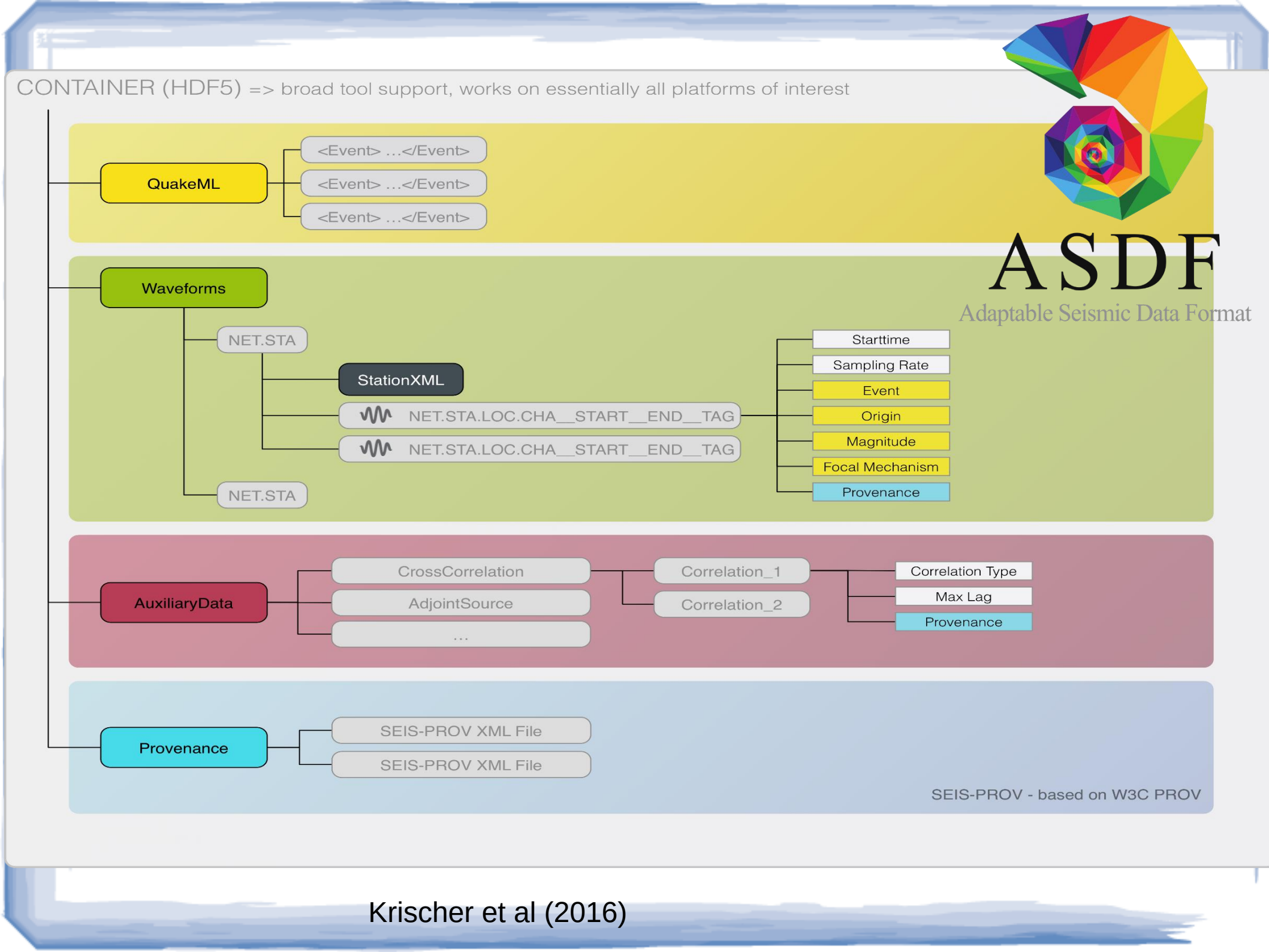

Krischer et al (2016)

Multiscale collaborative global Earth model

A framework that combines model parameterization, numerical solver, model refinement (workflow)

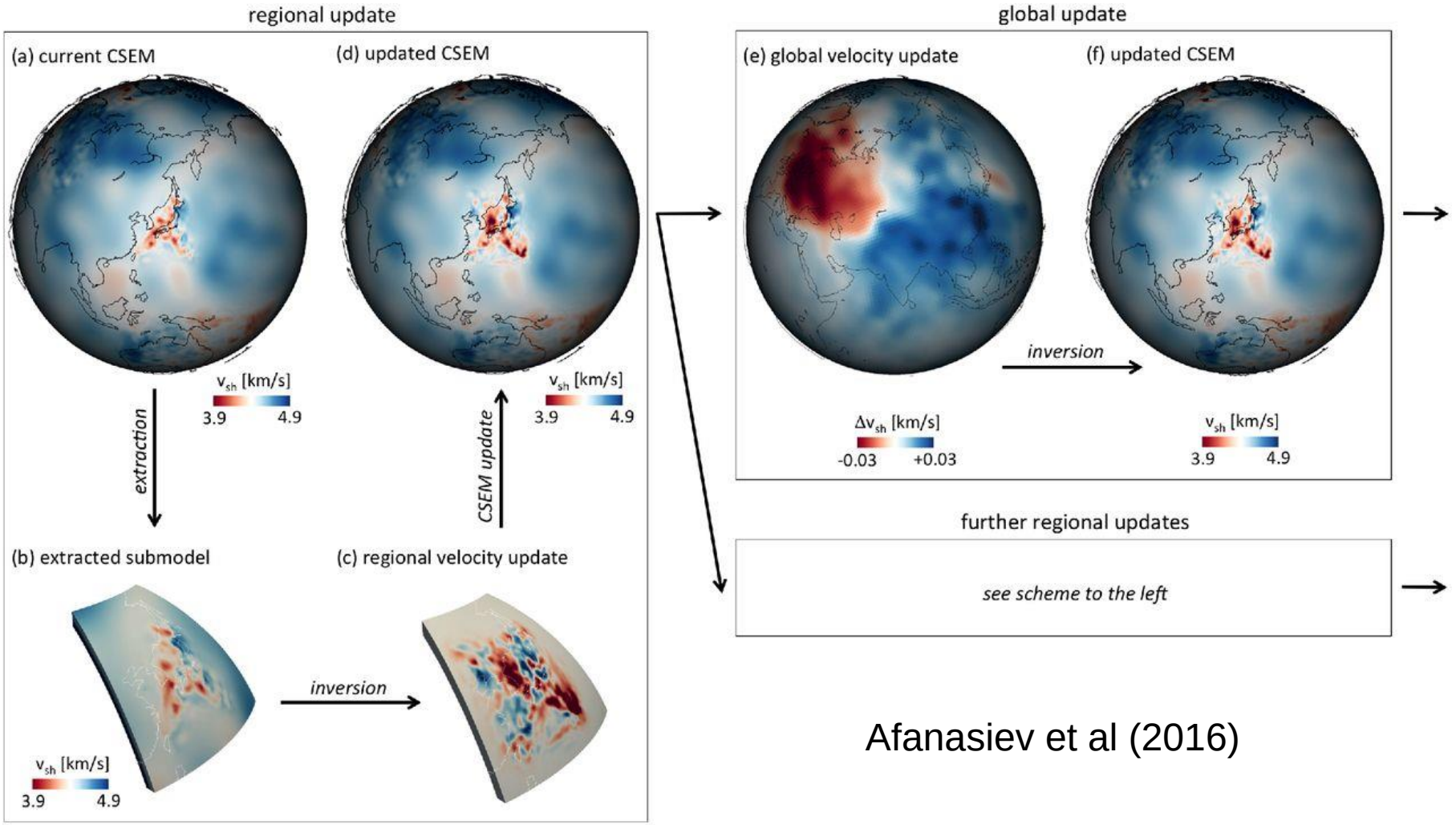

Afanasiev et al (2016)

PrincetonUniversity / **seisflows**

Watch 18 | Star 13 | Fork 12

Code | Issues 12 | Pull requests 0 | Pulse | Graphs

full waveform inversion and adjoint tomography workflows http://seisflows.readthedocs.org/en/latest/

936 commits | **1** branch | **0** releases | **6** contributors

Branch: **master** | New pull request | New file | Find file | HTTPS | https://github.com/Prin | Download ZIP

DmBorisov fixe muting — Latest commit 4e54267 14 days ago

docs	updated public_html paths	17 days ago
scripts	updated scripts/sfexamples	a month ago
seisflows	fixe muting	14 days ago
tests	refactored import_all	21 days ago
.gitignore	removed unused coverage metrics	2 months ago
.travis.yml	removed unused coverage metrics	2 months ago
LICENSE	edited docs	a year ago
README.md	updated README	a month ago

README.md

SeisFlows

SeisFlows is an open source seismic inversion package that

- Delivers a complete, customizable waveform inversion workflow
- Provides a framework for research in regional, global, and exploration seismology

Smith et al 2015

Alternative Approaches

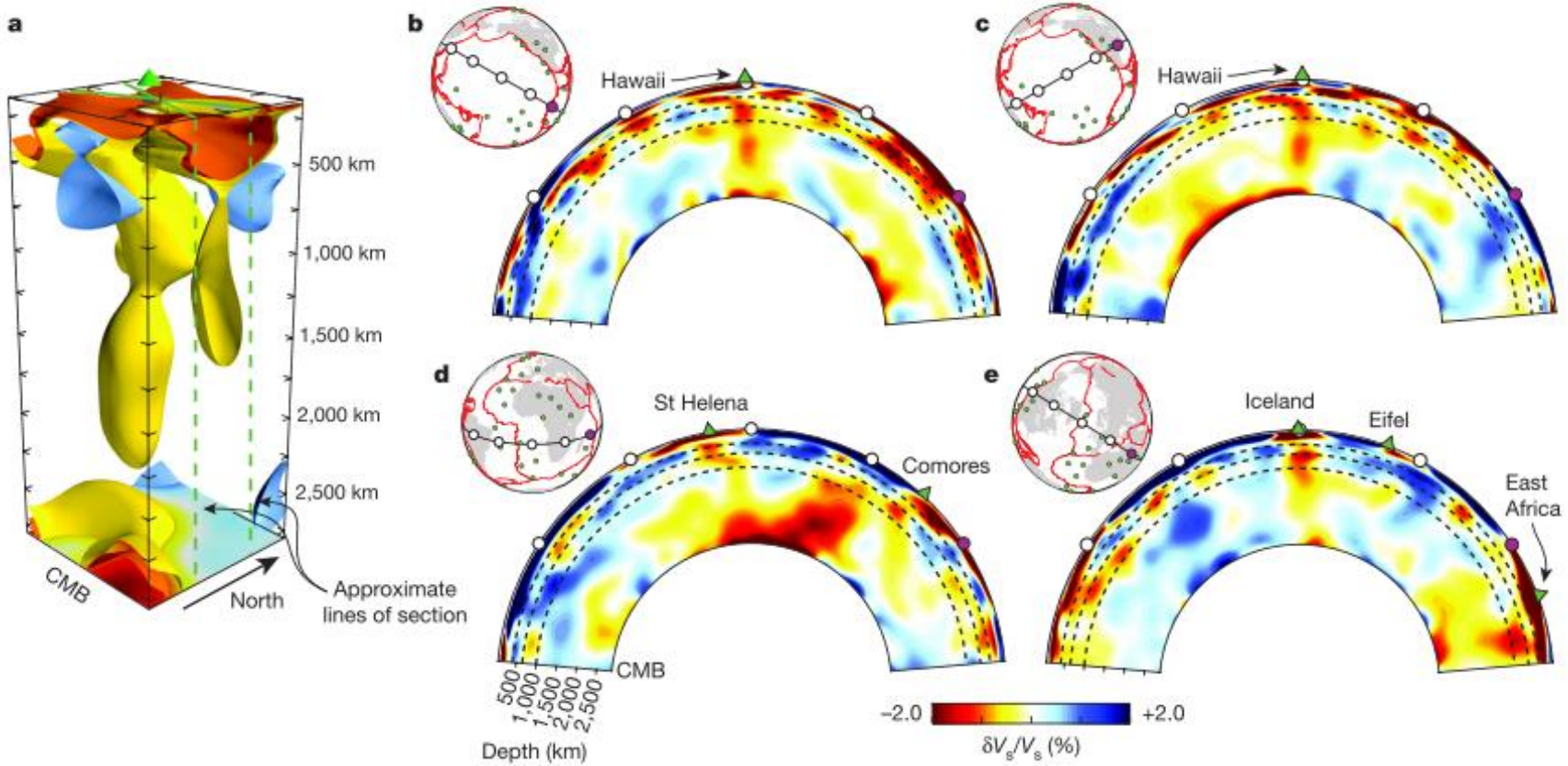

* 3D greens functions (numerical solver) for misfit functions, asymptotic (NACT) kernels.

French & Romanowicz (2015)

FWI applied around the globe

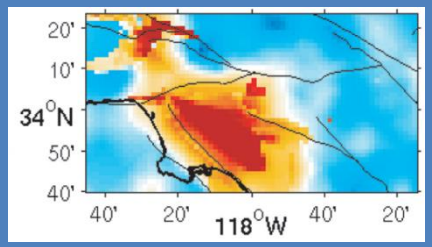

Chen et al (2007)
LA basin

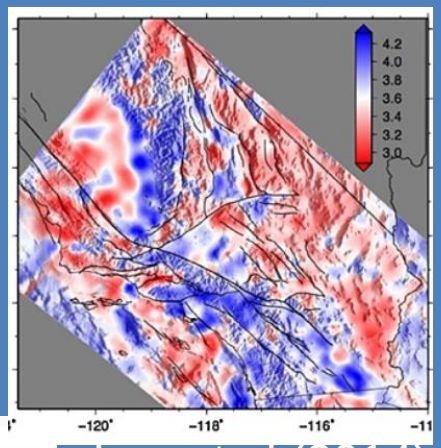

Lee et al (2014)
Socal crust

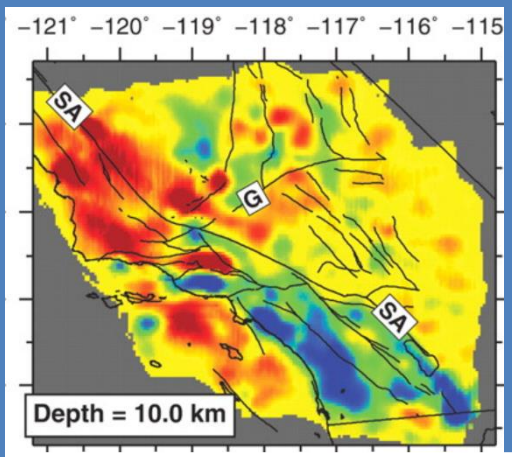

Tape et al (2009)
Socal Crust

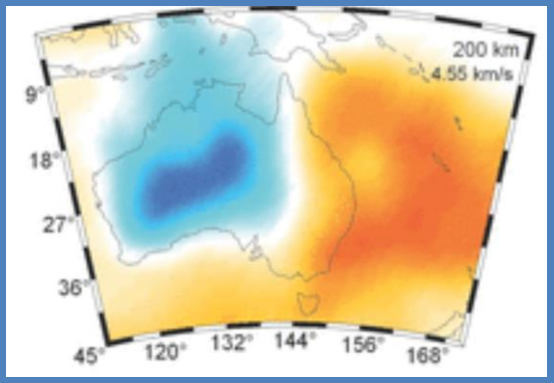

Fichtner et al (2009)
Australasian UM

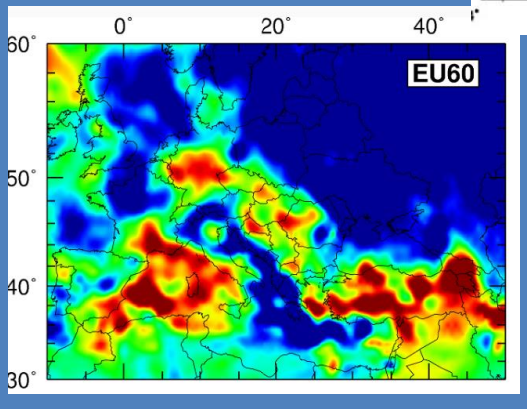

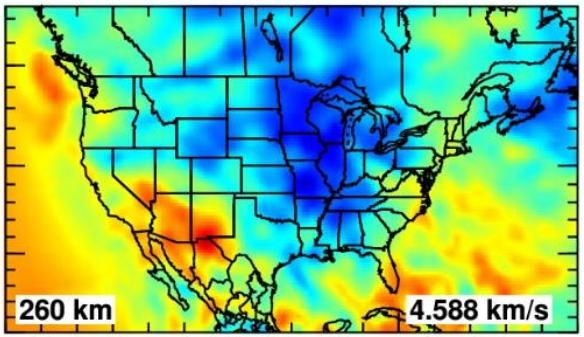

Zhu et al (2015, 2017) European & NAm

Dronning Maud Land

Lambert Graben

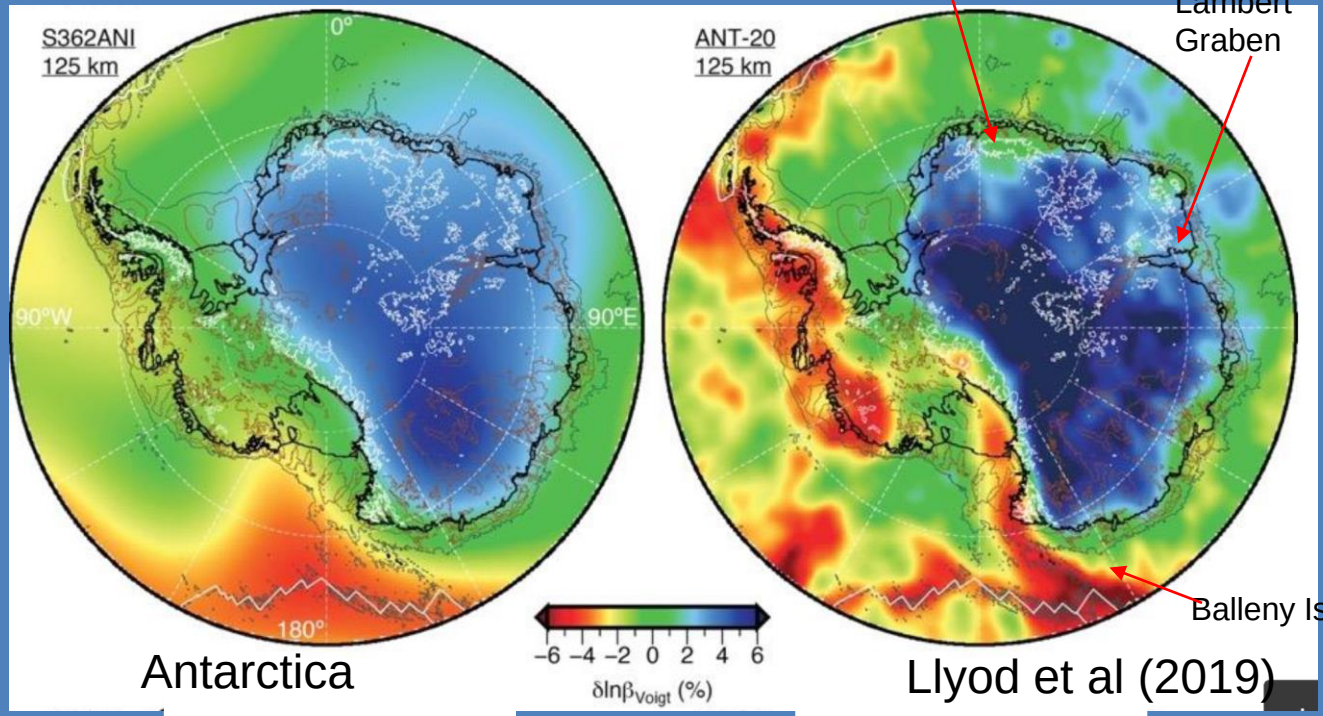

Balleny Is

Antarctica

Llyod et al (2019)

Adjoint tomography for the whole globe

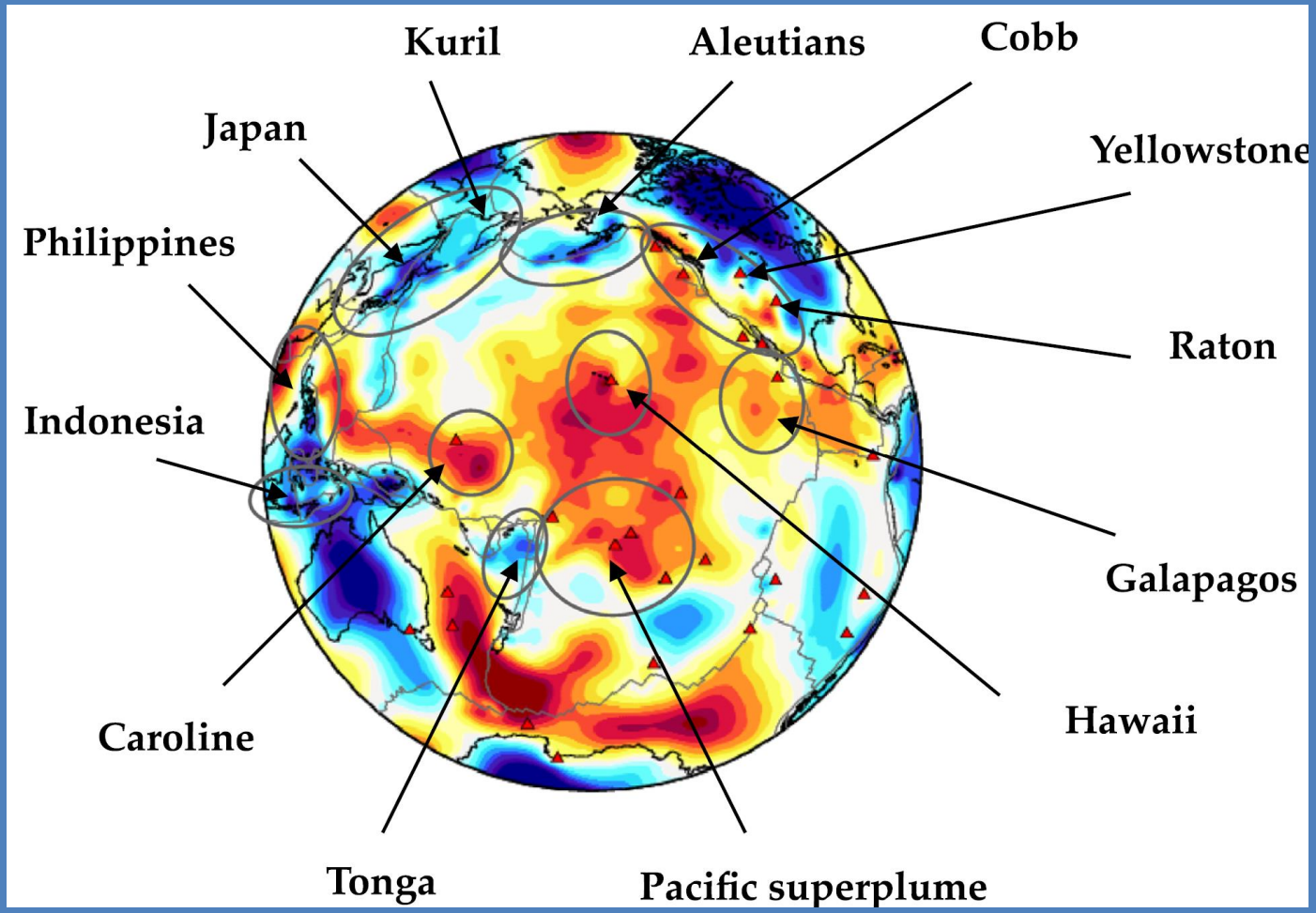

Slabs and plumes/hotspots enhanced in GLAD-M15 (Bozdag et al 2016)
New-generation GLAD-M25 (Lei et al 2019) with six-fold increase of data

Work-flow based Automatic FWI

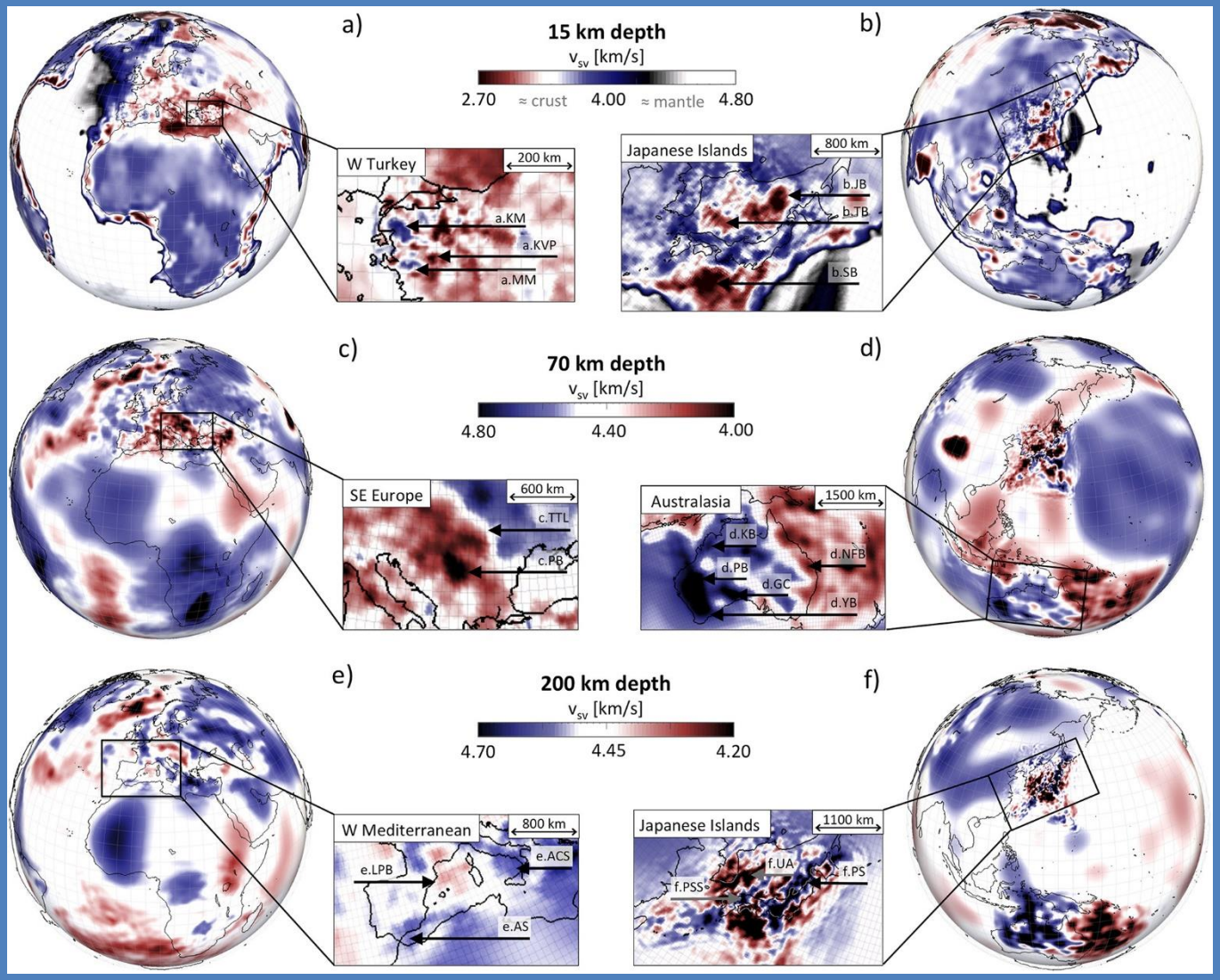

Automated Large-Scale Full Seismic Waveform Inversion: The Collaborative Seismic Earth Model (Fichtner et al, 2018)

Opportunities and Challenges

- Taking advantage of the ever-growing seismic array deployment and leveragi
- However, FWI at the scale of continents and the globe is still numerical extrem

It requires continued community-based effort on software development and maintenance, and methodology advances (optimization, inversion strateg

Future development of FWI for earthquake seismology

- Continued deployment of regional stations and arrays
- New datasets (ambient-noise)
- Special signals (scattered waves)
- Apply full numerical simulations to improve source characterization.

More data: Array deployments

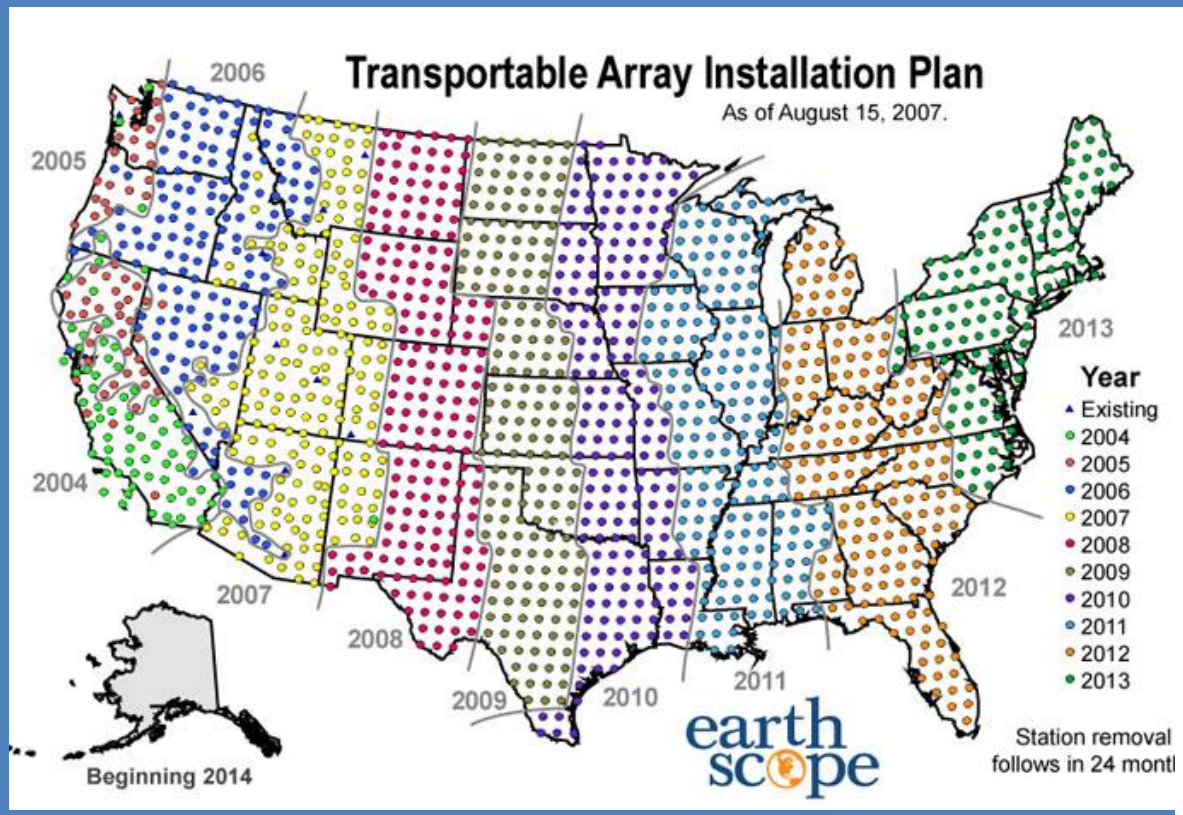

USArray Transportable Array deployment currently at Alaska

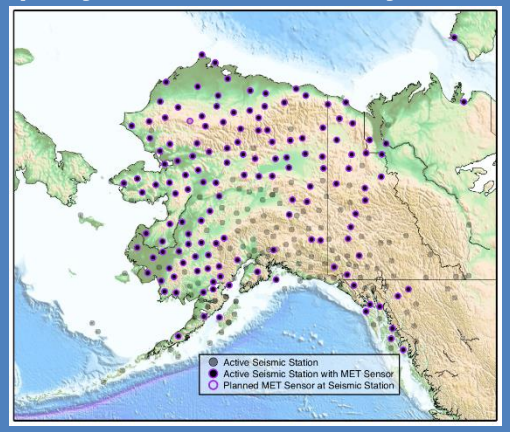

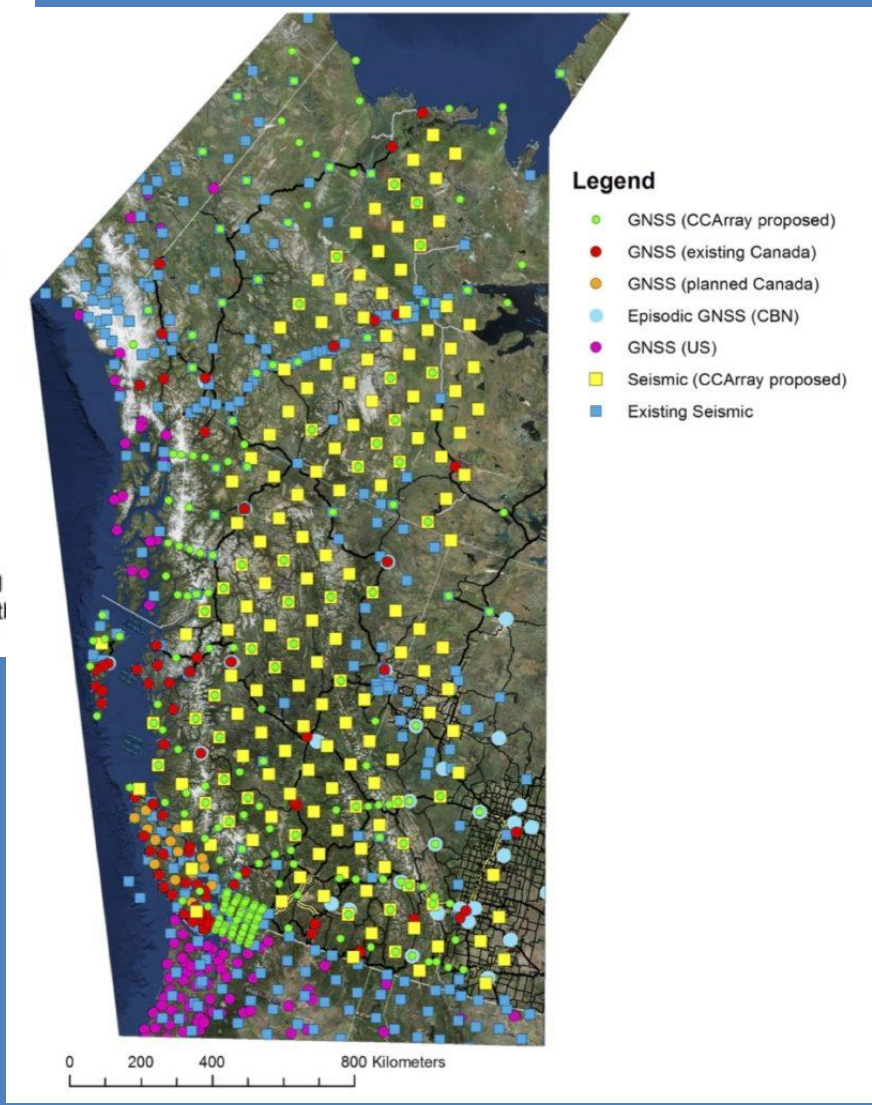

Canadian Cordillera Array (CCArray)
www.ccarray.org

FWI of ambinent-noise empirical Greens function

Ambient seismic field

⇩

Extract impulse response

$$\widehat{ANIRF}(x_A, x_B, \omega) = \left\langle \frac{\hat{v}(x_B, \omega)\hat{v}^*(x_A, \omega)}{\|\hat{v}(x_A, \omega)\|^2} \right\rangle$$

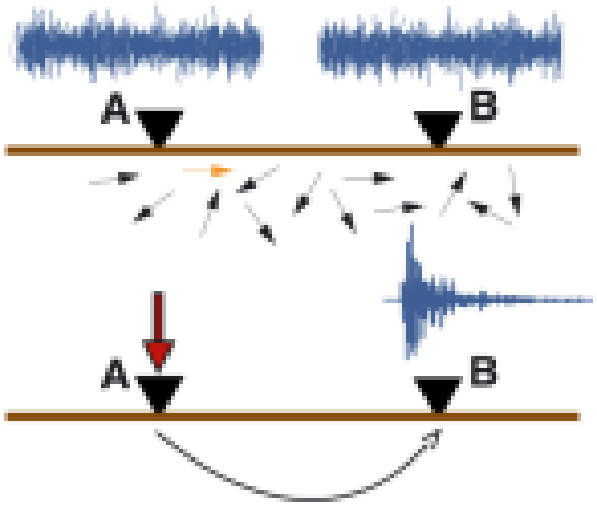

(From denolle et al., JGR, 2013)

Surface waves from cross-correlations of ambient seismic noise across the USArray

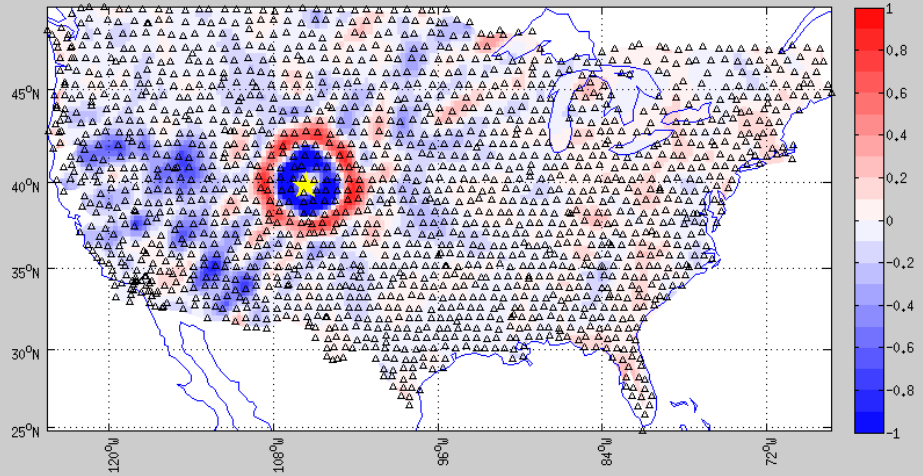

50–100 s

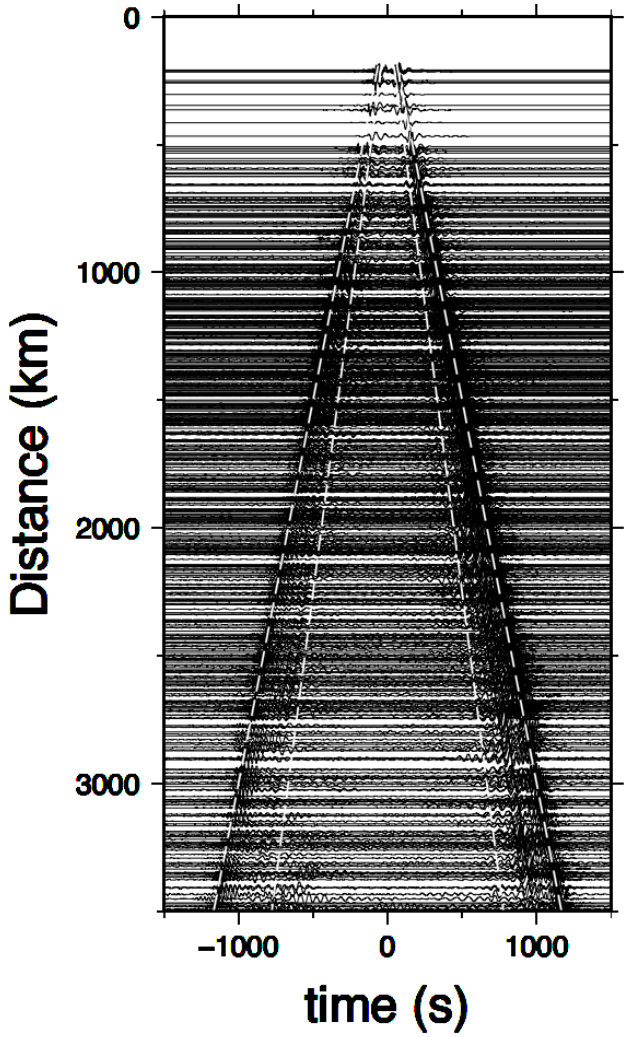

Anisotropic adjoint tomography in southern California

Interpretation of mid-lower crustal radial anisotropy

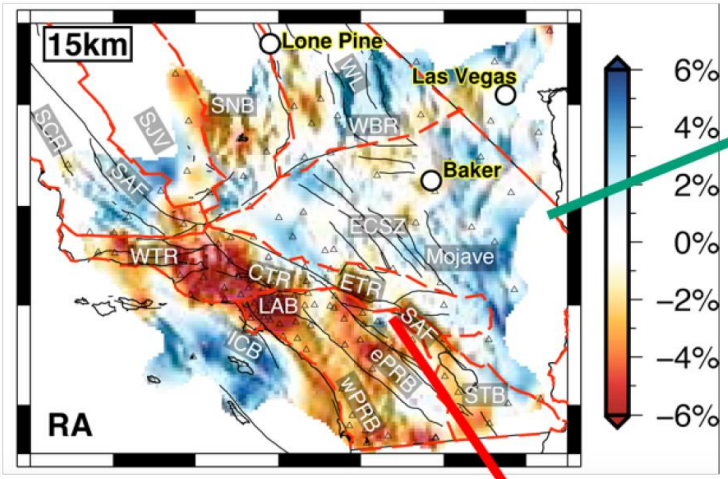

Oblique zone of negative radial anisotropy (-6%) bounded by Pacific coast and San Andreas Fault probably due to steeply dipping amphibole or horizontally aligned plagioclase associated with compressional tectonics.

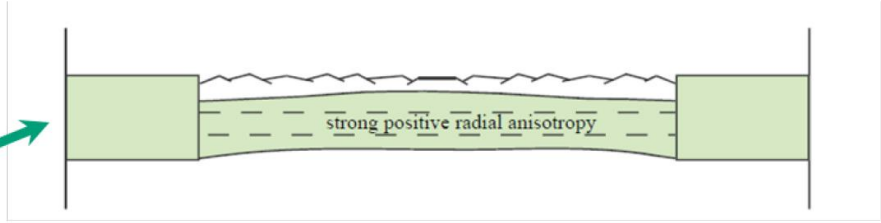

❑ Positive radial anisotropies might result from subhorizontally alignment of minerals in schists or genesis associated with extensional tectonics.

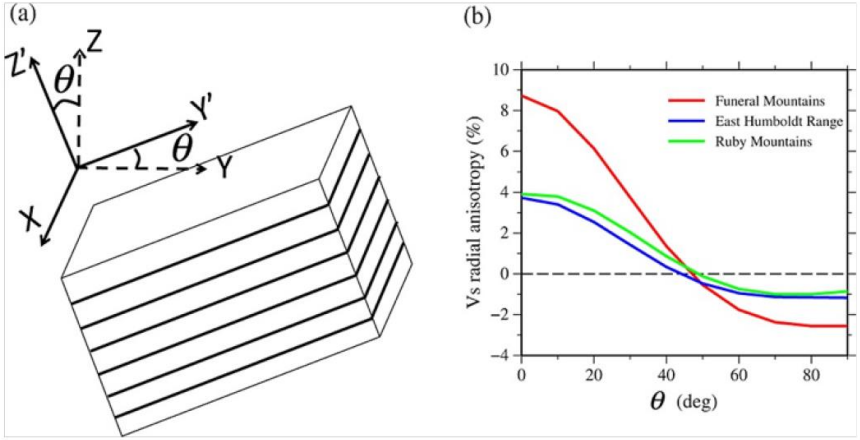

Vs radial anisotropies, $\gamma = (Vsh - Vsv)/Vs$, plotted as a function of rotation angle ϑ (Xie et al., 2013)

Wang et al (2019)

What about linear arrays?

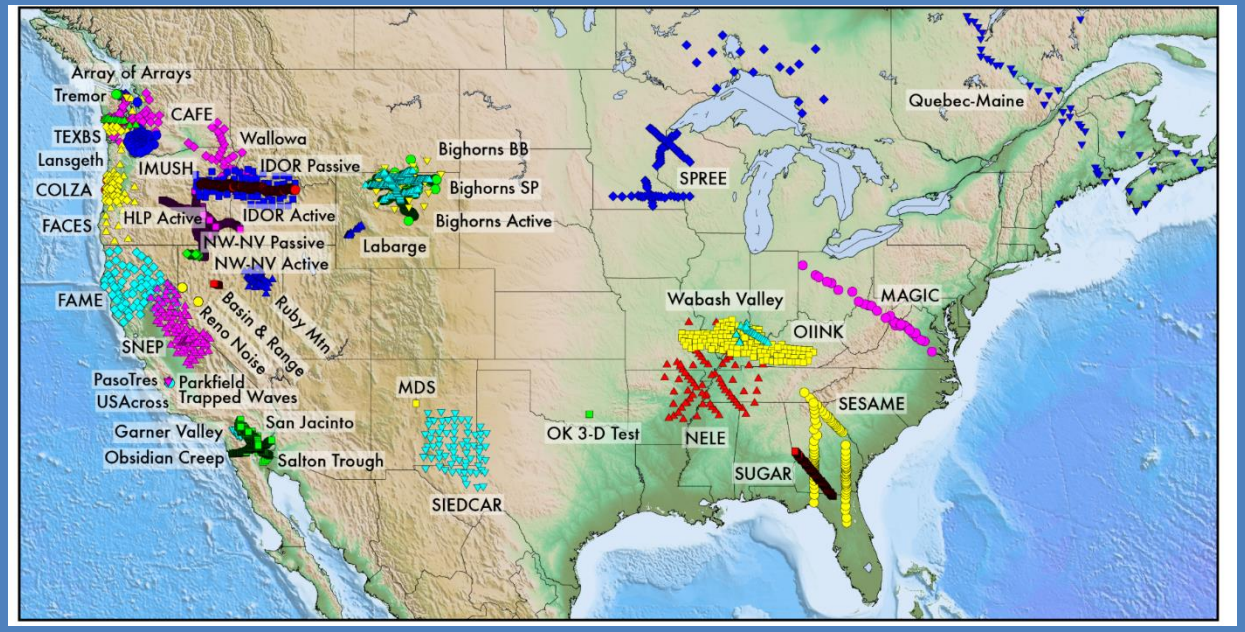

USArray: Flexible array experiments

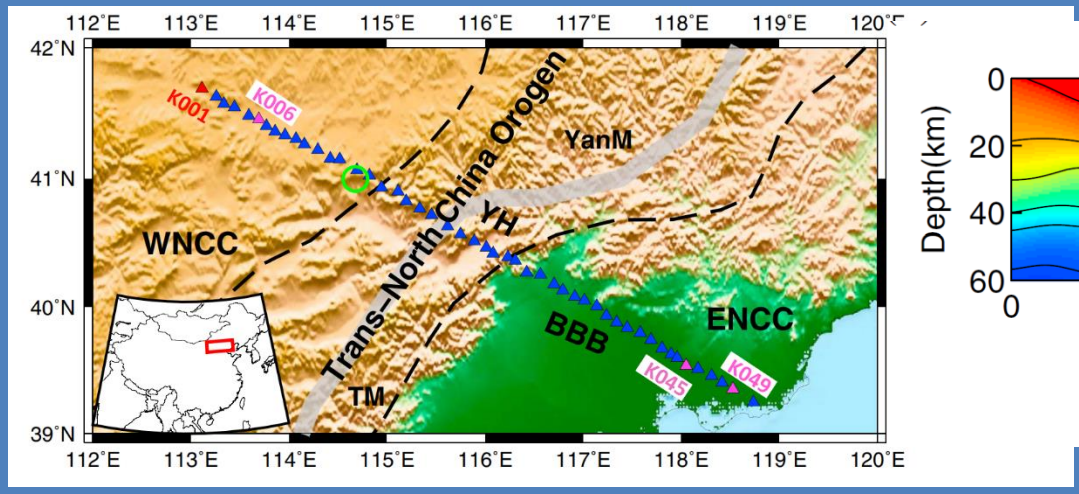

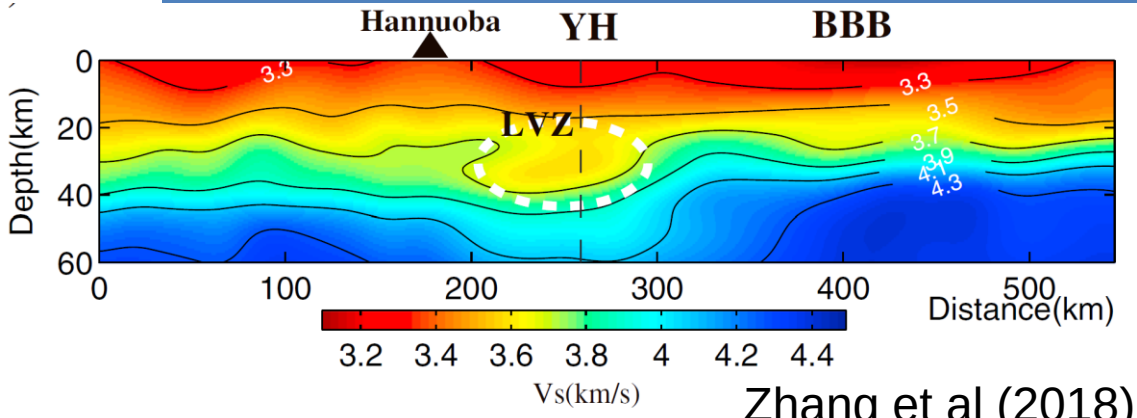

Zhang et al (2018)

Linear Array Ambient Noise Adjoint Tomography Reveals Intense Crust-Mantle Interactions in North China Craton: using a 3D/2D transformation for ambinent-noise EGFs.

Other Dataset: teleseismic body waves

* Noise cross-correlate functions

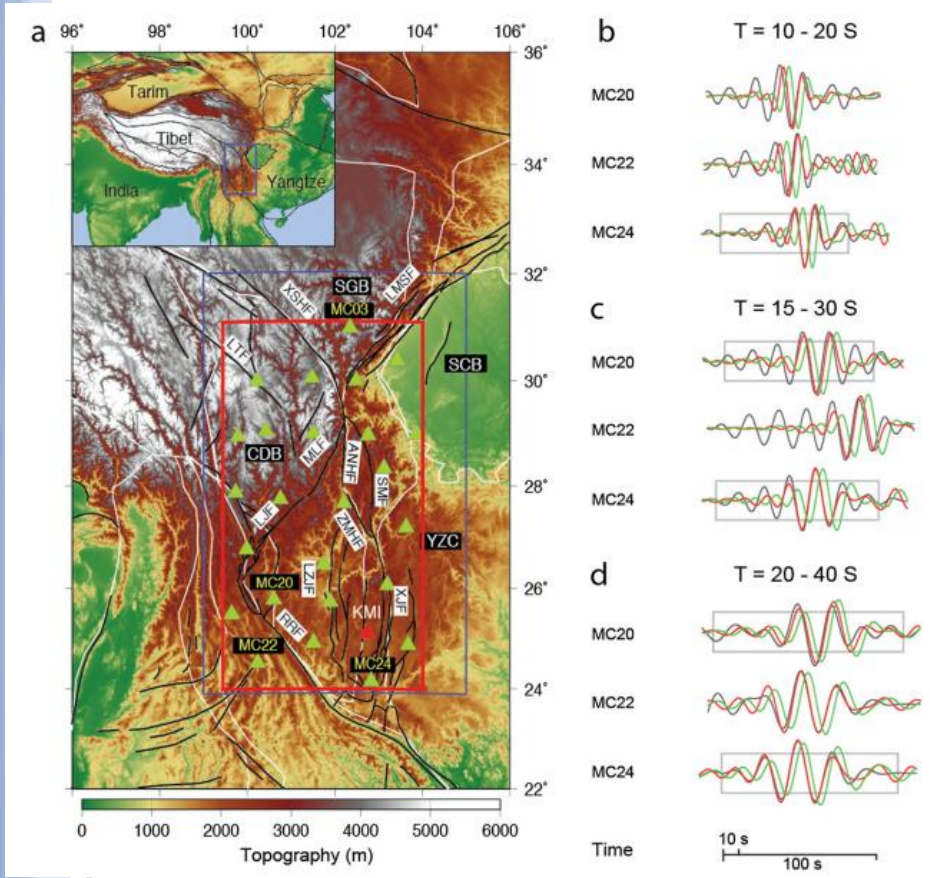

Chen et al. (2014), SE Tibet

scattered waves of teleseismic waves

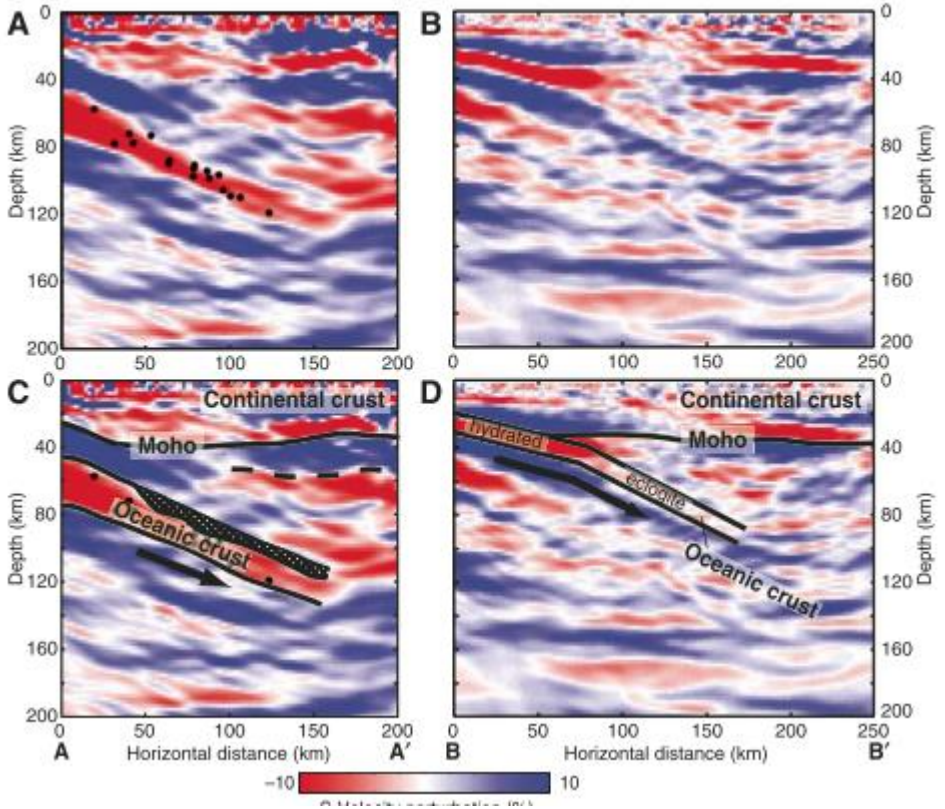

Rondenay (2008) GRT of scattered/converted waves of teleseismic P phase.

Scattering imaging based on FWI and hybrid methods

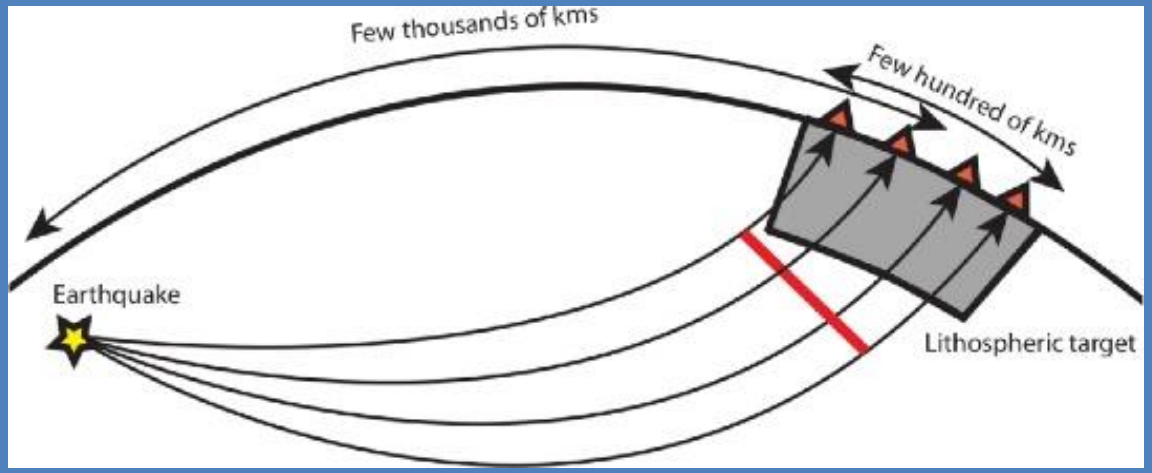

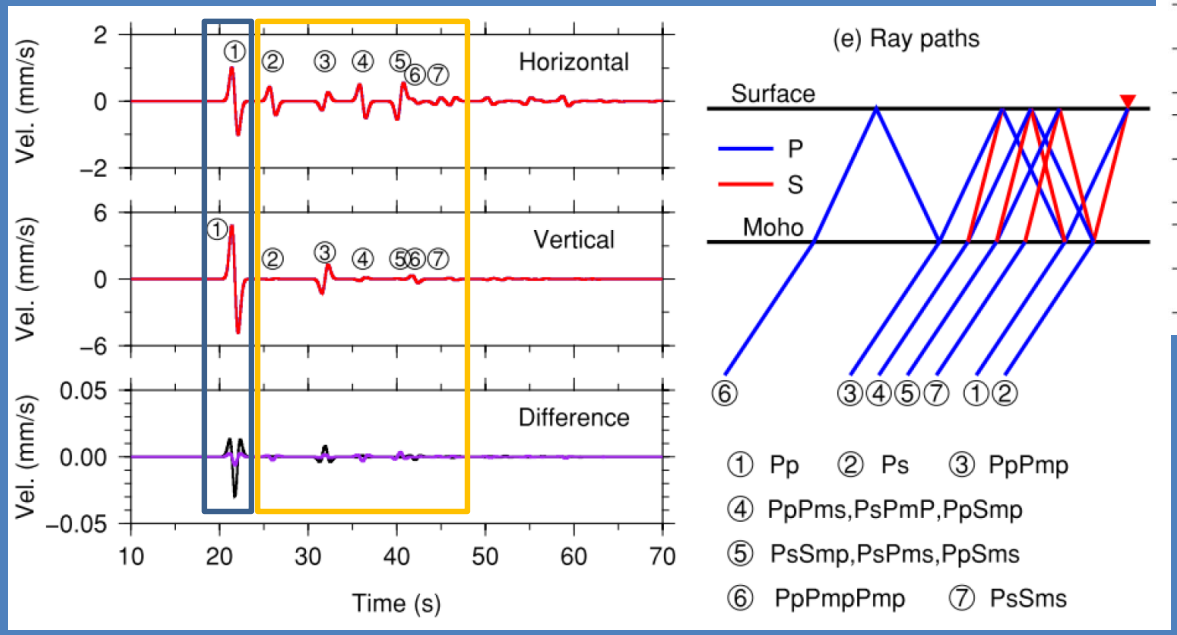

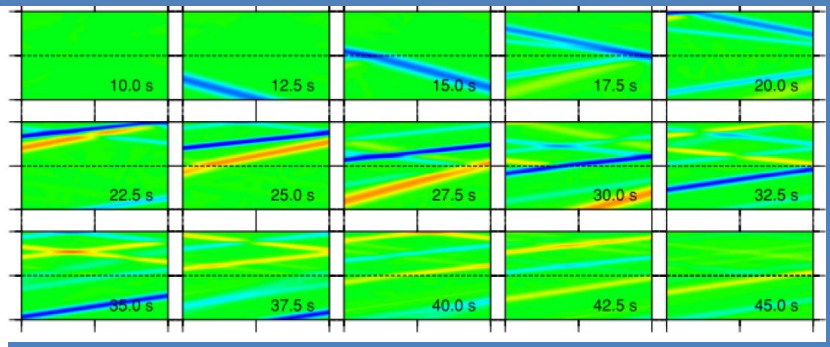

SEM-FK hybrid methods (Tong et al 2014)
External solver: Finite-wavenumber for 1D background model
Internal solver: full 3D SEM

FWI of teleseismic body waves based on DSM-SEM hybrid methods

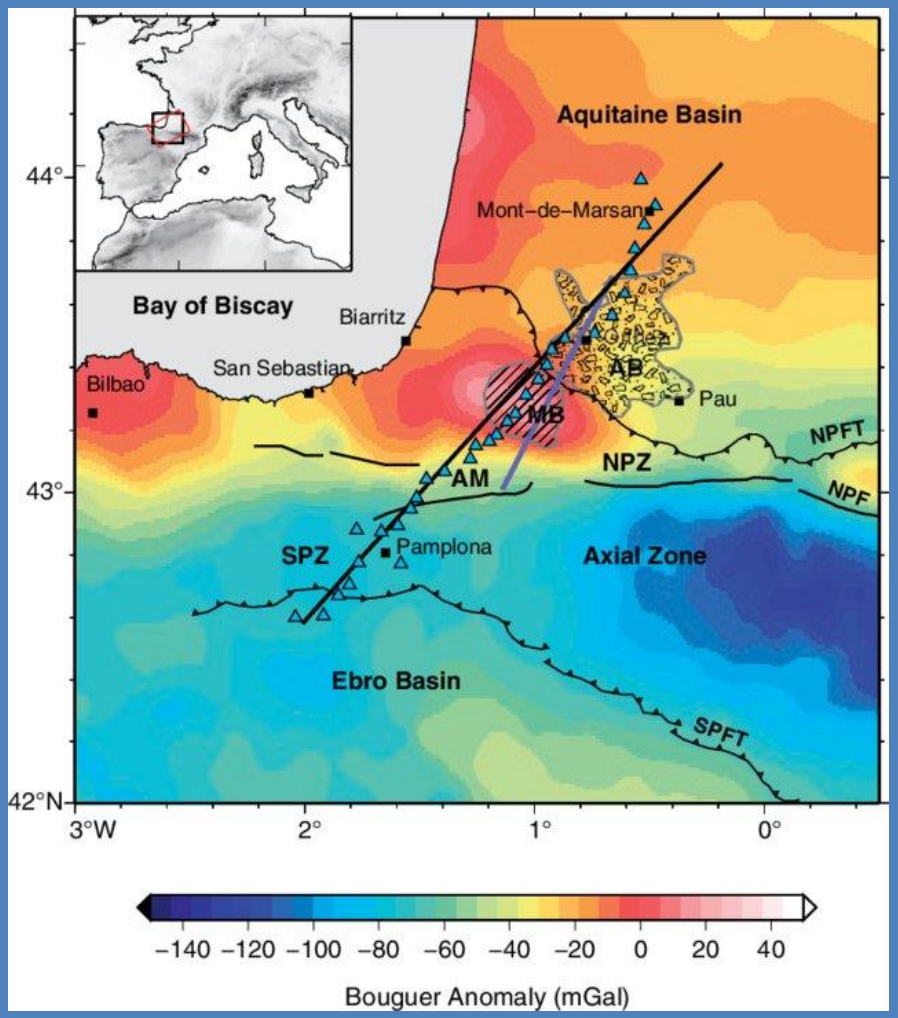

The deep roots of the western Pyrenees revealed by full waveform inversion of teleseismic P waves along PYROPE seismic transect (Wang et al 2016)

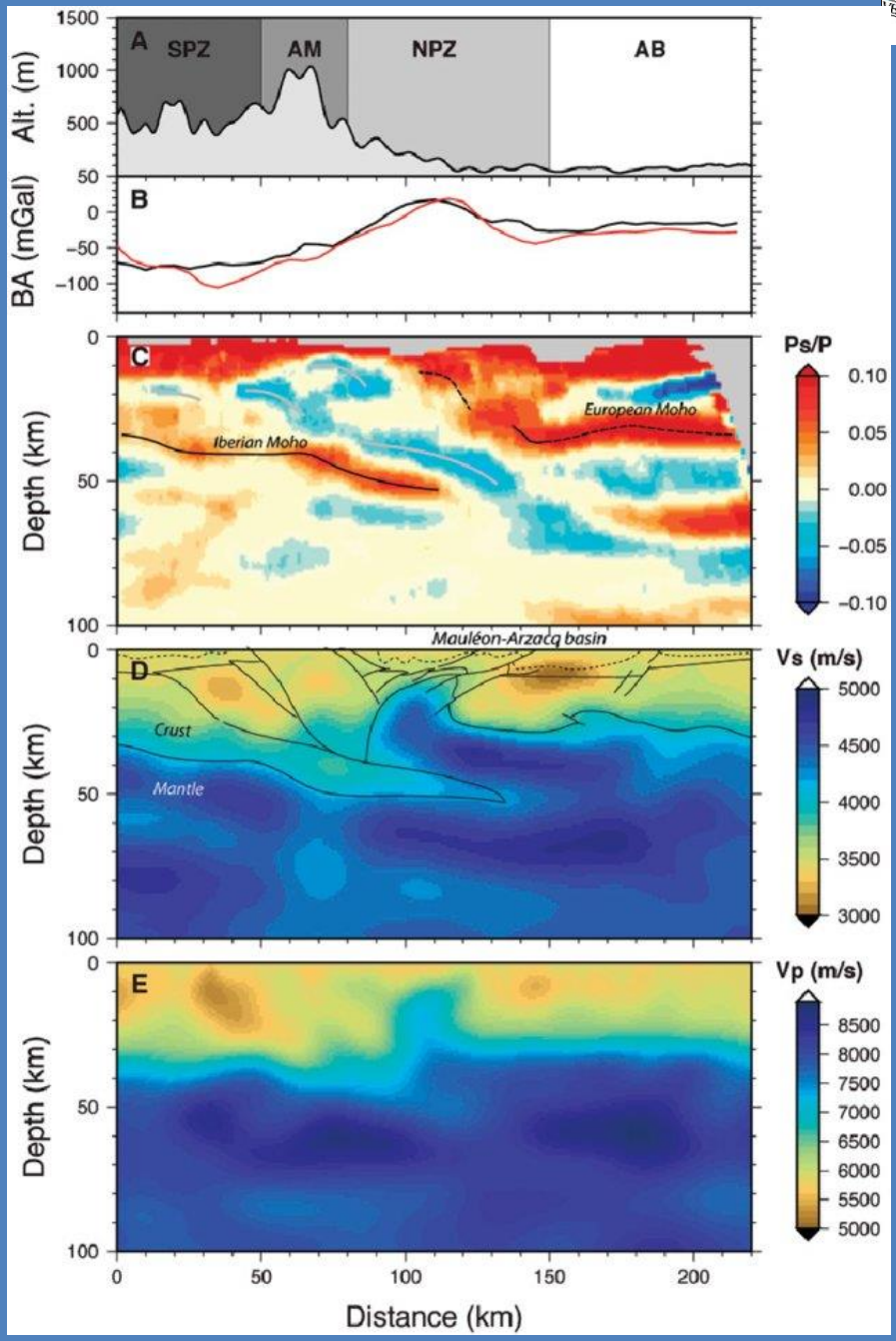

Conclusions

* Seismic imaging is transitioning from traditional tomographic methods (ray-based traveltime) to full-waveform inversions (FWI) based on sensitivity kernels computed by full numerical simulations of seismic wave propagation.

* In combination with the expanding deployment of global and regional seismic network as well as temporary arrays, FWI provides unprecedented high-resolution and robust images of the Earth's interior at global, regional and industrial scales.

* The continued incorporation of innovative datasets (ambient-noise surface-waves, teleseismic scattered waves, etc) will further improve the coverage and hence the seismic image quality.

* The future of high-resolution imaging: High-performance computing + more seismic dataset + innovative inversion strategies + continued software development by the community

"Full-waveform inversion (FWI) has emerged as the final and ultimate solution to the Earth resolution and imaging objective."

--Announcement of the 2013 SEG workshop on FWI

Acknowledgement:

Graduate students: Chuangxin Lin, Xin Song, Mostafa Khorshidi, Talha Qadri, Ding Liang, Elliott Sales de Andrade, Na Wang, Lin Zheng

Postdocs: Kai Wang, Piero Basini, Ping Tong

Collaborators: Carl Tape, Min Chen, Jeroen Tromp, Dimitri Komatitisch, Chao Zhang, Daniel Peter, Vala Hjorleifsdottir, Peter Shearer, Guy Masters, Shu-Huei Hung, Giovanni Grasselli, Qi Zhao, Shian-Jong Lee, C. A. Rychert and many others.

NSERC CRSNG

UNIVERSITY OF TORONTO

INNOVATION.CA
CANADA FOUNDATION FOR INNOVATION | FONDATION CANADIENNE POUR L'INNOVATION

SciNet
ADVANCED RESEARCH COMPUTING at the UNIVERSITY OF TORONTO

compute • calcul
CANADA

Ontario Research Fund

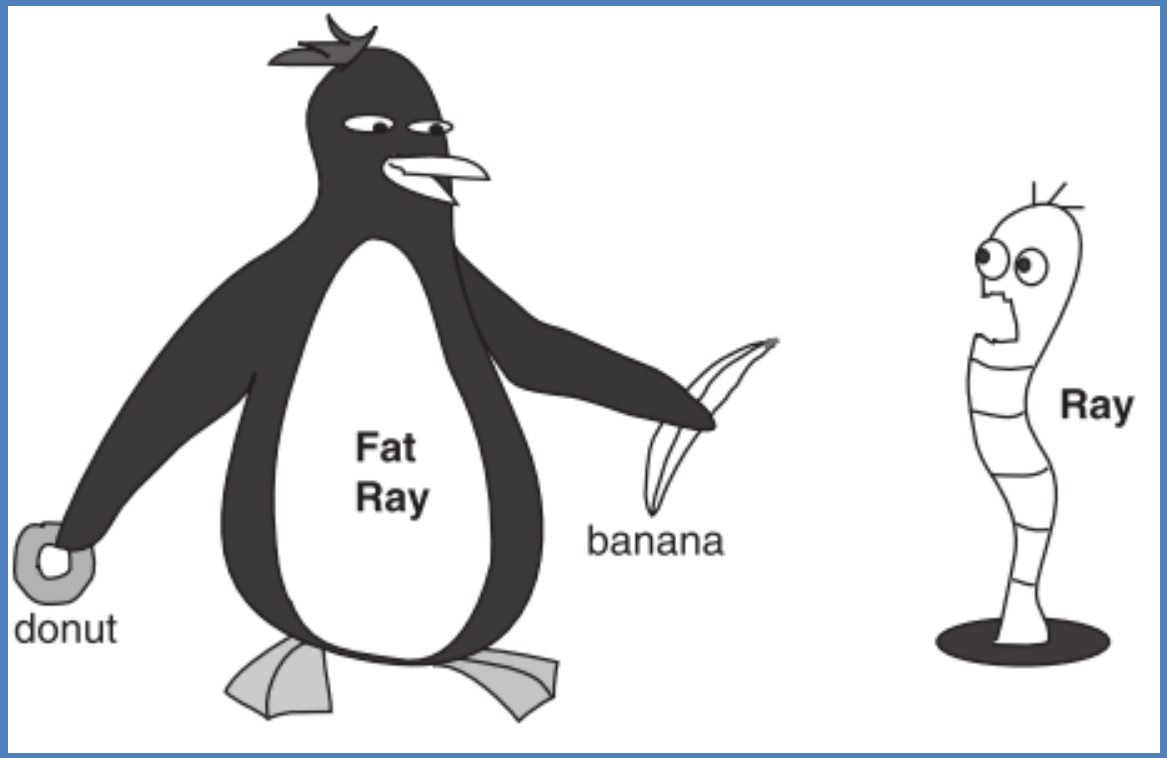

The End